

# **Advanced Optical Modulation Formats in High-speed Lightwave System**

by

Sen Zhang

Submitted to the Department of Electrical Engineering and Computer Science and the Faculty of the Graduate School of the University of Kansas in partial fulfillment of the requirements for the degree of Master of Science

---

Professor in Charge

---

---

Committee Members

---

Date thesis accepted

*Dedicated to my dear parents and sister*

## **ACKNOWLEDGEMENTS**

I would like to thank my advisor Professor Ronqing Hui, for his guidance in this thesis, and his support and valuable suggestions during my graduate study at the University of Kansas. He has taught me a lot, not limited in academic area. Also I would like to thank Professor Chris Allen and Professor John Gauch for their advices for my thesis and tutoring in my graduate study.

I would also like to thank two PhD students, Biao Fu and Yueting Wan, in our laboratory. Without their support, my graduate study in the Lightwave Telecommunications Laboratory will not be smooth and great.

I would like to thank my friends, Minnan Fei and Yuan Zhang, for their spiritual support through my study abroad. I appreciate their help and encouragement so much.

There are so many people I would like to thank. When I think of them, I would like to say “thank you” from the bottom of my heart.

## **ABSTRACT**

In the next generation of lightwave systems, high speed datarate like 10Gb/s or 40Gb/s per channel is very attractive. In addition, to pack more channels into one single fiber, channel spacing is decreased from 200GHz to 50GHz or even smaller. The direct side-effect is that linear and nonlinear degrading effects will be severe in such high-speed lightwave systems. An optimal modulation format which is more tolerant to linear and nonlinear impairments is needed urgently.

In this thesis, we will detail and compare several different modulation formats in high speed datarate lightwave systems. Five modulation formats are under research: NRZ-OOK, RZ-OOK, CS-RZ, NRZ-DPSK, and RZ-DPSK. First of all, system performance of modulation formats over several existing transmission fibers are compared in both 10Gb/s and 40Gb/s WDM systems. We found that the dominant degrading effect is dependent on datarate; also the choice of optimal fiber is dependent on modulation formats and datarate. Then, a simplified first-order rule concerning of SPM effect is extracted from series of numerical simulations of several modulation formats; in addition, RZ-DPSK is found to be the most tolerant to SPM degrading effect among the investigated modulation formats. Last, we show a 40Gb/s experimental testbed. Based on this testbed, CS-RZ and NRZ have been realized. These researches in both numerical methods and experiments give us an insight view of advanced modulation formats and provide a foundation for future research.

# TABLE OF CONTENTS

<b>1. INTRODUCTION.....</b>	<b>1</b>
<b>2. SIGNAL PROPAGATION IN OPTICAL FIBERS .....</b>	<b>5</b>
2.1. OVERVIEW .....	5
2.2. LINEAR AND NON-LINEAR EFFECTS IN FIBER.....	8
2.2.1. <i>Optical Loss</i> .....	8
2.2.2. <i>Chromatic Dispersion</i> .....	10
2.2.3. <i>SPM &amp; XPM</i> .....	12
2.2.4. <i>SRS &amp; SBS</i> .....	13
2.2.5. <i>FWM</i> .....	15
<b>3. OVERVIEW OF MODULATION FORMATS.....</b>	<b>17</b>
3.1. INTRODUCTION .....	17
3.2. GENERATION AND CHARACTERISTICS OF SEVERAL MODULATION FORMATS.....	18
3.2.1. <i>NRZ-OOK</i> .....	18
3.2.2. <i>RZ-OOK</i> .....	21
3.2.3. <i>NRZ-DPSK</i> .....	23
3.2.4. <i>RZ-DPSK</i> .....	27
3.2.5. <i>CS-RZ</i> .....	29
<b>4. IMPACT OF MODULATION FORMATS ON DIFFERENT FIBERS.....</b>	<b>33</b>
4.1. MOTIVATION.....	33
4.2. SCHEMATIC OF SYSTEM SETUP .....	33
4.3. COMPUTER SIMULATION MODEL .....	39
4.4. SIMULATION RESULTS .....	40
4.4.1. <i>40 Gb/s Optical systems</i> .....	41
4.4.2. <i>10 Gb/s Optical Systems</i> .....	47
4.5. CONCLUSION.....	50

<b>5. IMPACT OF MODULATION FORMATS ON DISPERSION-MANAGED OPTICAL SYSTEMS – A SIMPLIFIED MODEL.....</b>	<b>54</b>
5.1. MOTIVATION.....	54
5.2. SYSTEM SETUP AND NUMERICAL MODEL.....	55
5.3. SIMULATION RESULTS AND DISCUSSION.....	59
5.4. IMPACT OF ASE NOISE.....	63
5.5. CONCLUSION.....	69
<b>6. 40GB/S OPTICAL TRANSMISSION TESTBED.....</b>	<b>70</b>
6.1. MOTIVATION.....	70
6.2. 40GB/S TDM OPTICAL TRANSMISSION SYSTEM TESTBED.....	70
6.3. 40GB/S OPTICAL SYSTEM WITH NRZ MODULATION FORMAT.....	73
6.4. 40GB/S OPTICAL SYSTEM WITH CS-RZ MODULATION FORMAT.....	75
6.5. CONCLUSION.....	79
<b>7. CONCLUSION AND FUTURE WORK.....</b>	<b>81</b>
<b>REFERENCES.....</b>	<b>83</b>

## LIST OF FIGURES

Fig. 1.1 Increase in BL product over the developing lightwave systems. Different symbols are used to distinguish each generation. [Ref. 1] .....	1
Fig. 2.1 Measured loss profile of a single-mode fiber. Dashed curve shows the intrinsic loss profile resulting from Rayleigh scattering and absorption in pure silica. ....	9
Fig. 2.2 Measured variation of dispersion parameter D with wavelength for a single-mode fiber (revised from Figure 2.2 in Ref. [3]) .....	12
Fig. 2.3 Additional frequencies generated through FWM .....	15
Fig. 3.1 Block diagrams of NRZ transmitter (Ref. [6]) .....	20
Fig. 3.2 Optical spectrum NRZ signal with 10 Gbps of datarate.....	21
Fig. 3.3 Block diagrams of RZ transmitter (Ref. [6]) .....	22
Fig. 3.4 Optical spectrum of RZ signal with 10 Gbps of datarate .....	23
Fig. 3.5 Block diagrams of NRZ-DPSK (a) transmitter and (b) receiver (Ref. [6]) .....	26
Fig. 3.6 Optical spectrum of NRZ-DPSK signal with 10Gbps of datarate.....	26
Fig. 3.7 Block diagrams of RZ-DPSK transmitter (Ref. [6]).....	28
Fig. 3.8 Optical spectrum of RZ-DPSK signal with 10Gbps of datarate.....	28
Fig. 3.9 Block diagrams of CS-RZ transmitter and signal generation (Ref. [6]).	30
Fig. 3.10 Optical spectrum of CS-RZ signal with 10 Gbps of datarate .....	31
Fig. 4.1 Schematic of WDM system setup (Ref. [6]) .....	37
Fig. 4.2 Dispersion management in simulation .....	38
Fig. 4.3 NRZ in 40 GHz systems, 3dBm per-channel average power (Ref. [6]) (a) Single Channel and (b) 40- $\lambda$ WDM with 100GHz channel spacing.....	42
Fig. 4.4 CS-RZ in 40 GHz systems, 3dBm per-channel average power (Ref. [6]) (a) Single Channel and (b) 40- $\lambda$ WDM with 100GHz channel spacing .....	43
Fig. 4.5 NRZ-DPSK in 40 Gb/s systems, 0dBm per-channel average power (Ref. [6]) (a) Single Channel and (b) 40- $\lambda$ WDM with 100GHz channel spacing .....	44

Fig. 4.6 RZ-DPSK in 40 GHz systems, 0dBm per-channel average power (Ref. [6]) (a) Single Channel and (b) 40- $\lambda$ WDM with 100GHz channel spacing .....	46
Fig. 4.7 Comparison between SMF-28 and LEAF fibers in a single channel 10 GHz system, 3dBm per-channel average power. (a) NRZ , (b) CS-RZ, (c) NRZ-DPSK and (d) RZ-DPSK (Ref. [6]).....	48
Fig. 4.8 160- $\lambda$ , 10Gb/s systems with 25GHz channel spacing and -3dBm per-channel average power: (a) NRZ, (b) CS-RZ, (c) NRZ-DPSK and (d) RZ-DPSK (Ref. [6]) .....	49
Fig. 5.1 Block Diagram of System Setup .....	56
Fig. 5.2 Dispersion management in the simulation.....	57
Fig. 5.3 EOP of signal evolves over the transmission distance, with 12dBm average input power and NRZ format .....	59
Fig. 5.4 SPM-limited transmission distance versus launched optical power for 10Gb/s data rate. Scattered points: results of numerical simulations. Solid lines: linear fittings between $\log(L_{SPM})$ and $P(\text{dBm})$ with the slope of $-1$ . .....	62
Fig. 5.5 SPM-limited transmission distance versus launched optical power for 40Gb/s data rate. Scattered points: results of numerical simulations. Solid lines: linear fittings between $\log(L_{SPM})$ and $P(\text{dBm})$ with the slope of $-1$ . .....	63
Fig. 5.6 SPM-limited transmission distance versus launched optical power for 10Gb/s data rate. Scattered points: results of numerical simulations. Solid lines: linear fittings between $\log(L_{SPM})$ and $P(\text{dBm})$ with the slope of $-1$ . Dashed lines: ASE-limited transmission distance from analytical equation. ....	67
Fig. 5.7 SPM-limited transmission distance versus launched optical power for 40Gb/s data rate. Scattered points: results of numerical simulations. Solid	

lines: linear fittings between  $\log(L_{SPM})$  and  $P(\text{dBm})$  with the slope of  $-1$ .

Dashed lines: ASE-limited transmission distance from analytical equation.

.....	68
Fig. 6.1 40Gb/s optical testbed using electrical MUX/DEMUX (Ref. [10]).....	71
Fig. 6.2 10G to 40G multiplexing in electrical domain (Ref. [10]).....	72
Fig. 6.3 40G to 10G demultiplexing in electrical domain (Ref. [10]) .....	73
Fig. 6.4 Eye diagrams measured at: (A) back-to-back, (B) 2km, (C) 5km and (D) 8km without dispersion compensation; and (E) 10km with dispersion compensation . (Ref. [10]) .....	74
Fig. 6.5 40Gb/s optical system with CS-RZ modulation (Ref. [10]).....	77
Fig. 6.6 Measured optical spectrum of CS-RZ signal. (Ref. [10]).....	77
Fig. 6.7 CS-RZ eye diagram measured at (A) back-to-back, (B) after 10km SMP without DCF and (C) after 10km with DCF. (Ref. [10]).....	79

## LIST OF TABLES

TABLE 4.1: SYSTEM PARAMETERS (REF. [6]).....	38
TABLE 4.2: PHYSICAL PARAMETERS OF ALL KINDS OF FIBER (REF. [6]) .....	39
TABLE 4.3: SUMMARY OF COMPARISON BETWEEN DIFFERENT FORMATS OVER DIFFERENT FIBERS ...	51
TABLE 5.1: FIBER PARAMETERS IN THE SIMULATION .....	56
TABLE 5.2: POWER- $L_{SPM}$ PRODUCT $C$ FOR DIFFERENT MODULATION FORMATS IN [ $mW \cdot km$ ] (REF [7]).....	61

# 1. Introduction

The use of light as communication methods can date back to antiquity if we define optical communications in a broader way [1]. People had used mirrors, fire beacons, or smoke signals to convey a single piece of information. The modern fiber-optic communications started around 1970s when GaAs semiconductor laser was invented and the optical fiber loss could be reduced to 20 dB/km in the wavelength region near  $1\mu\text{m}$  [1]. Since then, fiber-optic communication has rapidly developed. The enormous progress of lightwave systems can be grouped into several generations. A widely used figure of merit is the bit rate-distance product,  $BL$ , where  $B$  is the bit rate and  $L$  is the repeater spacing. Fig. 1.1 shows the increase of bit rate-distance product over the developing of lightwave systems. These data are quantified through various laboratory experiments [1].

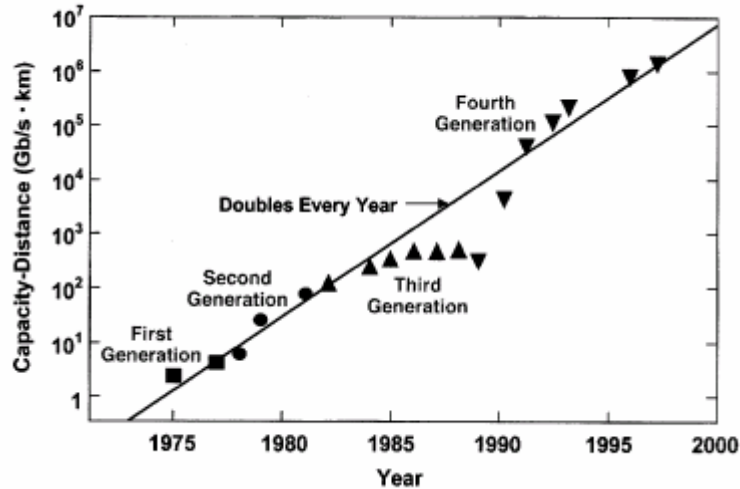


**Fig. 1.1** Increase in  $BL$  product over the developing lightwave systems. Different symbols are used to distinguish each generation. [Ref. 1]

The first generation of lightwave systems was commercially available in 1980. It operated near 800 nm and used GaAs semiconductor lasers. The data rate of the lightwave systems could reach 45 Mb/s with repeater spacing up to 10 km.

The second generation of lightwave systems became commercially available in late 1980s. It operated in the wavelength region near  $1.3\mu\text{m}$ , where fiber loss is below 1 dB/km and optical fiber has exhibited minimum dispersion in this region. From the early 1980s, the developments of InGaAsP semiconductor lasers and detectors operating near  $1.3\mu\text{m}$  and the use of single-mode fibers have contributed to the availability of the second generation of lightwave systems. By 1987, the second-generation lightwave systems with data rate of 1.7 Gb/s and a repeater spacing of 50 km were available.

The third-generation lightwave systems with data rate of 2.5 Gb/s became commercially available in 1990. It was known that silica fibers had the minimum loss (0.2-dB/km) near the wavelength  $1.55\mu\text{m}$ . Unfortunately there is large fiber dispersion near  $1.55\mu\text{m}$ . To overcome this problem, dispersion-shifted fiber and single-longitudinal-mode lasers were developed. Drawback of the third-generation lightwave system was that the signal has to be electronically regenerated periodically with the repeater spacing of typically from 60 to 70 km.

Use of erbium-doped fiber amplifiers (EDFA) and wavelength-division multiplexing (WDM) is the distinct character of fourth-generation lightwave system. EDFA was developed in 1985 and was commercially available in 1990. EDFA made it possible to transmit optical signals up to tens of thousands of kilometer without

using electronic regenerator. The advent of WDM technique started a revolution and increased the capacity of lightwave system enormously. By 1996, commercial transatlantic and transpacific cable systems became available. A demonstration of optical transmission over 11,300 km using actual submarine cables at a data rate of 5Gb/s [1] was realized in the same year. Since then, many submarine lightwave systems have been developed worldwide.

The next generation of lightwave system, the fifth-generation of lightwave system has been under development for a while. The emphasis of research can be commonly categorized into two groups. One emphasis is to extend the wavelength range to L-band (1570nm – 1610nm) and S-band (1485nm – 1520nm) to increase the number of channels in WDM. Currently lightwave systems are operating in the conventional wavelength window, known as C-band, which is from 1530 nm to 1565 nm. Another emphasis is to increase the data rate of each channel. Many experiments have been done operating at data rate of 10 Gb/s or 40 Gb/s since year 2000. In such higher data rate lightwave systems, dispersion compensation management and combating of nonlinearity degrading effects like SPM, XPM and FWM are becoming urgent. In this issue, modulation formats has been a key factor.

As we will describe detailedly in the following parts of this thesis, when the data rate of lightwave systems are increasing to 10Gb/s or 40Gb/s, optical signals are more sensitive to the linear and nonlinear degrading effects. Consequently, NRZ that has been used for a long time in lightwave system is no more an optimal modulation format in the next generation of lightwave system. A modulation format that is more

tolerant to linear and nonlinear impairments is needed. The capacity of lightwave system, bit rate-distance product, will be improved dramatically using optimal modulation formats compared to NRZ format. In addition, spectral efficiency would be improved using optimal modulation format thus more information could be conveyed per wavelength or more wavelengths can be co-propagated over fibers. In economical view, optimal modulation formats will permit service providers to develop their existing lightwave network without overall upgrade and to utilize the most of the existing systems; thus to save the expenses.

In this thesis, characteristics of several different modulation formats and their tolerance to linear and nonlinear impairments will be discussed. Valuable results and conclusions are provided for the high-speed lightwave systems.

## 2. Signal Propagation in Optical Fibers

### 2.1. Overview

The core of a lightwave system is optical fiber. When an optical signal transmits over a fiber, it suffers from linear and nonlinear degrading effects in the fiber. Those linear and nonlinear effects are properties of fibers. Before discussing system performance of advanced modulation formats it is necessary to talk about the properties of fiber. Optical loss or attenuation and chromatic dispersion are linear degrading effects; SPM (self-phase modulation), XPM (cross-phase modulation), FWM (four-wave mixing), SRS (stimulated Raman scattering) and SBS (stimulated Brillouin scattering) are nonlinear degrading effects. SRS and SBS are different from the other nonlinear effects because they originate from stimulated inelastic scattering not Kerr effect. Before getting into the detailed explanation of each degrading effect above, I would like to present one of the most fundamental equations, - nonlinear Schrödinger equation, which is often used to describe the signal propagation over optical fibers in single mode condition.

From Ref [2], a generalized nonlinear Schrödinger equation which describes the evolution of optical waveform at the transmission distance  $z$  is shown as the following:

$$\begin{aligned} \frac{\partial A}{\partial z} + \frac{\alpha}{2} A + \frac{i}{2} \beta_2 \frac{\partial^2 A}{\partial T^2} - \frac{1}{6} \beta_3 \frac{\partial^3 A}{\partial T^3} \\ = i\gamma \left[ |A|^2 A + \frac{i}{\omega_0} \frac{\partial}{\partial T} (|A|^2 A) - T_R A \frac{\partial |A|^2}{\partial T} \right] \end{aligned} \quad (2.1.1)$$

where  $T$  is a frame of reference moving with the pulse at the group velocity  $V_g$  and  $T = t - z/v_g = t - \beta_1 z$ ;  $|A|^2$  represents optical power;  $\gamma$  is the nonlinearity coefficient;  $\alpha$  is the attenuation constant;  $\beta_1$ ,  $\beta_2$  and  $\beta_3$  are the first order, second order and third order derivative of mode-propagation constant  $\beta$  about the center frequency  $\omega_0$ ;  $T_R$  is related to the slope of the Raman gain and is usually estimated to be  $\sim 5$  fs. Equation (2.1.1) includes the effects of fiber loss through  $\alpha$ , of chromatic dispersion through linear delay  $V_g$ , of nonlinear effects through  $\gamma$ . The term which is proportional to  $\beta_3$  accounts for the higher order of dispersion which becomes important for ultra-short pulses. The last two terms on the right-side of the equation are related to the effects of stimulated inelastic scattering such as SRS and SBS. The detailed information of these linear and nonlinear effects will be discussed in chapter 2.2.

Equation (2.1.1) is a nonlinear partial differential equation which generally does not have an analytical solution except for some special cases. A numerical approach is needed to understand the nonlinear effects in fibers most of time. Many of simulators use Split-Step Fourier Transform (SSFT) to simulate the evolution of optical waveform over fiber. In a standard SSFT method, fiber span is divided into many short sections and the dispersion operator and the nonlinear operator are treated separately in each section (Ref. [6]). If we rewrite the Equation (2.1.1) like this (Ref. [2, 6]):

$$\frac{\partial A(z, T)}{\partial z} = (\hat{D} + \hat{N})A \quad (2.1.2)$$

where  $\widehat{D}$  and  $\widehat{N}$  are dispersion operator and nonlinear operator respectively.

They are given by:

$$\widehat{D} = -\frac{i\beta_2}{2} \frac{\partial^2}{\partial T^2} + \frac{1}{6} \beta_3 \frac{\partial^3}{\partial T^3} - \frac{\alpha}{2} \quad (2.1.3)$$

$$\widehat{N} = i\gamma \left[ |A|^2 + \frac{i}{\omega_0 A} \frac{\partial}{\partial T} (|A|^2 A) - T_R \frac{\partial |A|^2}{\partial T} \right] \quad (2.1.4)$$

From Equation (2.1.2), we can get the evolution of the complex optical field along the fiber from one section to the next section:

$$A(z + h_n, T) = \exp(h_n \widehat{N}) \exp(h_n \widehat{D}) A(z, T) \quad (2.1.5)$$

Where  $h_n$  is the length of the  $n^{\text{th}}$  fiber section.

The execution of linear dispersion operator  $\exp(h_n \widehat{D})$  can be carried out in frequency domain, so we can write:

$$\exp(h_n \widehat{D}) A(z, T) = F^{-1} \left\{ \exp[h_n \widehat{D}(i\omega)] F[A(z, T)] \right\} \quad (2.1.6)$$

Where  $\widehat{D}(i\omega) = \frac{i\beta_2}{2} \omega^2 - \frac{\alpha}{2}$  is the dispersion operator in Fourier domain and

$F$  and  $F^{-1}$  denote the Fourier and inverse Fourier transformations respectively. Finally, for SSFT numerical method, the equation for the optical field evolution can be written as following:

$$A(z + h_n, T) = \exp(h_n \widehat{N}) F^{-1} \left\{ \exp[h_n \widehat{D}(i\omega)] F[A(z, T)] \right\} \quad (2.1.7)$$

In Equation (2.1.7), the dispersion acts with optical signal first in frequency domain, and nonlinear effects interfere with optical signal in time domain separately.

In general, the simulation using SSFT starts with the known waveform at the

transmitter  $A(0,T)$  and finds the optical field of each consecutive fiber section till the end of the transmission.

## 2.2. Linear and Non-linear Effects in Fiber

### 2.2.1. Optical Loss

Optical loss is an important parameter for fiber. When optical signal transmits over fiber, its power is lost due to material absorption and Rayleigh scattering. The expression of fiber loss is shown as following:

$$P_T = P_0 \exp(-\alpha L) \quad (2.2.1)$$

where  $\alpha$  is called attenuation constant;  $P_0$  is the optical signal power at the input of a fiber of length  $L$ ; and  $P_T$  is the transmitted power. Usually fiber loss is expressed using units of dB/km by using the relation

$$\alpha_{dB} = -\frac{10}{L} \log \left[ \frac{P_T}{P_0} \right] = 4.343\alpha \quad (2.2.2)$$

Fig. 2.1 from Ref. [2] shows a measured profile of a single-mode fiber.

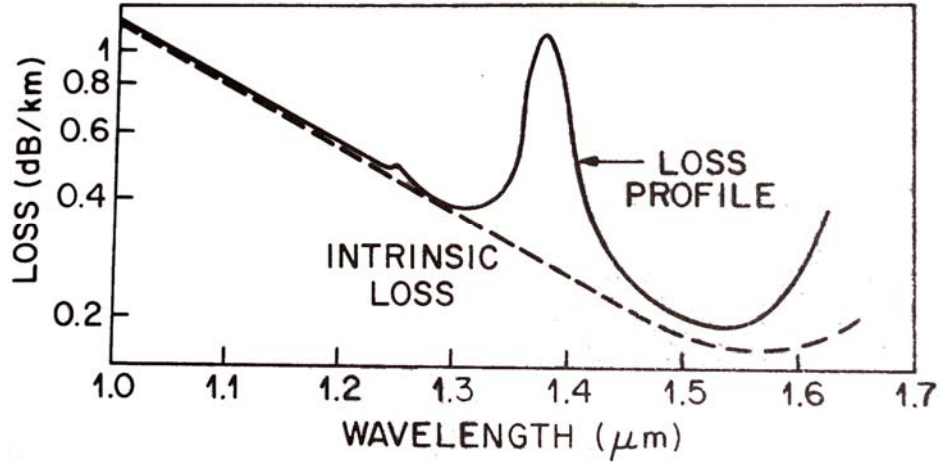


**Fig. 2.1 Measured loss profile of a single-mode fiber. Dashed curve shows the intrinsic loss profile resulting from Rayleigh scattering and absorption in pure silica.**

Fiber loss  $\alpha_{dB}$  is dependent on wavelength. Material absorption and Rayleigh scattering contribute to the loss dominantly.

The loss beyond  $2 \mu m$  is dominantly due to material absorption. Pure silica absorbs either in the ultraviolet region or in the far-infrared region beyond  $2 \mu m$ . However, there is significant absorption in the wavelength window  $0.5-2 \mu m$  due to the even small impurities of fiber. The small peak around  $1.23 \mu m$  and  $1.37 \mu m$  in Fig. 2.1 are caused by the material absorption due to impurities of fiber.

The Rayleigh scattering dominates in the short wavelength. Rayleigh scattering is a fundamental scattering mechanism arising from random density fluctuations frozen into the fused silica during manufacture. The intrinsic loss level (in dB/km) is estimated by the equation:

$$\alpha_R = \frac{C}{\lambda^4} \tag{2.2.3}$$

where the constant  $C$  is in the range of 0.7- 0.9  $dB/(km \cdot \mu m^4)$  depending on the constituents of the fiber core.

### 2.2.2. Chromatic Dispersion

Chromatic dispersion is very important among the degrading effects of fiber. The fundamental mechanism of chromatic dispersion is the frequency dependence of the refractive index  $n(\omega)$ . Because the velocity of light is determined by  $c/n(\omega)$  the different spectral components associated with the pulse would travel at different speeds. The dispersion-induced spectrum broadening would be very important even without nonlinearity. The effects of dispersion can be accounted for by expanding the mode-propagation constant  $\beta$  in a Taylor series about the center frequency  $\omega_0$ :

$$\beta(\omega) = n(\omega) \frac{\omega}{c} = \beta_0 + \beta_1(\omega - \omega_0) + \frac{1}{2} \beta_2(\omega - \omega_0)^2 + \dots \quad , \quad (2.2.4)$$

$$\text{where } \beta_m = \left[ \frac{d^m \beta}{d\omega^m} \right]_{\omega=\omega_0} \quad (m = 0, 1, 2, \dots) \quad (2.2.5)$$

so it is easy to get the first and second order derivatives from equation (2.2.4) and (2.2.5):

$$\beta_1 = \frac{1}{c} \left[ n + \omega \frac{dn}{d\omega} \right] = \frac{1}{v_g} \quad (2.2.6)$$

$$\beta_2 = \frac{1}{c} \left[ 2 \frac{dn}{d\omega} + \omega \frac{d^2 n}{d\omega^2} \right] \approx \frac{\lambda^3}{2\pi c^2} \frac{d^2 n}{d\lambda^2} \quad (2.2.7)$$

where  $c$  is the speed of light in vacuum.  $\lambda$  is the wavelength.

The wavelength where  $\beta_2 = 0$  is called zero-dispersion wavelength  $\lambda_D$ . However, there is still dispersion at wavelength  $\lambda_D$  and higher order dispersion will be considered in this case. Another parameter concerning the dispersion of fiber is more often used, which is often referred to as dispersion parameter  $D$ . The relationship between  $D$  and  $\beta_1, \beta_2$  is shown as following:

$$D = \frac{d\beta_1}{d\lambda} = -\frac{2\pi c}{\lambda^2} \beta_2 \approx -\frac{\lambda}{c} \frac{d^2 n}{d\lambda^2} \quad (2.2.8)$$

From Equation (2.2.8), we can see that  $D$  has opposite sign with  $\beta_2$ . Fig. 2.2 shows the measured variation of dispersion parameter  $D$  with wavelength for a single-mode fiber (Ref. [3]). In the regime where wavelength  $\lambda < \lambda_D$ ,  $\beta_2 > 0$  (or  $D < 0$ ), the fiber is said to exhibit normal dispersion. In the normal-dispersion regime, high-frequency components of optical signal travel slower than low-frequency components. By contrast, in the regime where wavelength  $\lambda > \lambda_D$ ,  $\beta_2 < 0$  (or  $D > 0$ ), fiber is said to exhibit anomalous-dispersion. In the anomalous-dispersion regime, high-frequency components of signal travel faster than low-frequency components. Soliton transmission is possible in the anomalous regime through a balance between the dispersive and nonlinear effects.

Dispersion plays an important role in signal transmission over fibers. The interaction between dispersion and nonlinearity is an important issue in lightwave system design.

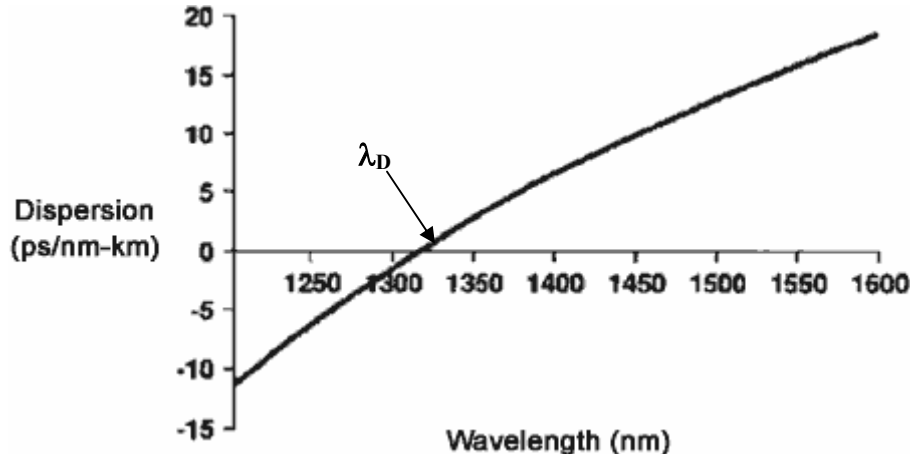


**Fig. 2.2 Measured variation of dispersion parameter D with wavelength for a single-mode fiber (revised from Figure 2.2 in Ref. [3])**

### 2.2.3. SPM & XPM

SPM (Self-phase modulation) and XPM (Cross-phase modulation) are the two most important nonlinear effects which originate from the intensity dependence of the refractive index.

SPM refers to the self-induced phase shift experienced by an optical field during its propagation in optical fibers.

XPM refers to the nonlinear phase shift of an optical field induced by a co-propagating field at a different wavelength.

When two optical fields at frequencies  $\omega_1$  and  $\omega_2$ , polarized along the  $x$  axis, co-propagate simultaneously inside the fiber:

$$E = \frac{1}{2} \hat{x} [E_1 \exp(-i\omega_1 t) + E_2 \exp(-i\omega_2 t) + c.c.] \quad (2.2.9)$$

Nonlinear phase shift for the field at  $\omega_1$  induced by SPM and XPM can be expressed as:

$$\phi_{NL} = n_2 k_0 L (|E_1|^2 + 2|E_2|^2) \quad (2.2.10)$$

where  $n_2$  is the nonlinear-index coefficient,  $k_0 = 2\pi/\lambda$  and  $L$  is the fiber length.

On the right-hand side of the Equation (2.2.10), the first term  $n_2 k_0 L |E_1|^2$  is the SPM-induced nonlinear phase shift; and the second term  $2n_2 k_0 L |E_2|^2$  is the XPM-induced nonlinear phase shift. So for equally intense optical fields, the contribution of XPM to the nonlinear phase shift is twice compared with that of SPM.

#### 2.2.4. SRS & SBS

Both SRS (Stimulated Raman scattering) and SBS (Stimulated Brillouin scattering) effects result from stimulated inelastic scattering in which the optical field transfers part of its energy to the nonlinear medium.

The main difference between SRS and SBS is that optical phonons participate in SRS while acoustic phonons participate in SBS. In a simple quantum-mechanical picture applicable to both SRS and SBS, a photon of the pump is annihilated to create a photon at the downshifted Stokes frequency and a phonon with the right energy and momentum to conserve the energy and the momentum. Of course, a higher-energy photon at the anti-Stokes frequency can also be created if a photon of right energy and momentum is available. Although SRS and SBS have the very similar origin, there is fundamental difference between them. SBS in optical fibers occurs only in the backward direction whereas SRS dominates in the forward direction.

For SRS, the initial growth of the Stokes wave can be described by a simple relation:

$$\frac{dI_s}{dz} = g_R I_p I_s \quad (2.2.11)$$

where  $I_s$  is the Stokes intensity,  $I_p$  is the pump intensity, and  $g_R$  is the Raman-gain coefficient.

A similar relation holds for SBS with  $g_R$  replaced by the Brillouin-gain coefficient  $g_B$ . Raman gain spectrum is very broad extending up to ~30 THz. The peak gain  $g_R$  is about  $10^{-13}$  m/W at a pump wavelength of 1  $\mu\text{m}$  and occurs at the Stokes shift of about 13 THz. By contrast, the Brillouin-gain spectrum is extremely narrow with a bandwidth about 10 MHz. The peak value of  $g_B$  is about  $6 \times 10^{-11}$  m/W and occurs at the Stokes shift around 10 GHz.

For both SRS and SBS, the significant conversion of pump energy of Stokes energy occurs only when the pump intensity exceeds a certain threshold level. Typically, SRS can be observed at a pump power of 1mW; while, SBS can be observed at the pump power of 10mW.

For SRS, its Stokes shift is so large (up to 13 THz) that it is larger than the whole bandwidth of our simulated WDM system in traditional C-band. For SBS, its narrow spectrum bandwidth is negligible compared to the optical spectrum of transmitted signal in high-speed lightwave system, e.g. 10/40 Gb/s. Thus, when we consider the nonlinear degrading effects of fibers, SRS and SBS are both ignored in this thesis's consideration.

### 2.2.5. FWM

Four-wave mixing (FWM) is a nonlinear process that occurs when two or more wavelength co-propagating in the same fiber and satisfying phase matching condition. A number of new frequencies are generated due to interaction of two or more frequencies in FWM. Suppose there are three frequencies ( $\omega_i, \omega_j, \omega_k$ ) co-propagating in the fiber, so the generation of new frequencies ( $\omega_{ijk}$ ) is given by:

$$\omega_{ijk} = \omega_i + \omega_j - \omega_k \quad (2.5.1)$$

If two of three frequencies are same therefore there are only two new wavelengths generated in fiber, as shown in Fig. 2.3. This phenomenon is also called partially degenerate four-wave-mixing (PDFWM) (Ref. [11]). In this case,  $\omega_i = \omega_j$ , and the generated additional frequencies are denoted as  $\omega_{112}$  and  $\omega_{221}$  in the Fig. 2.3.

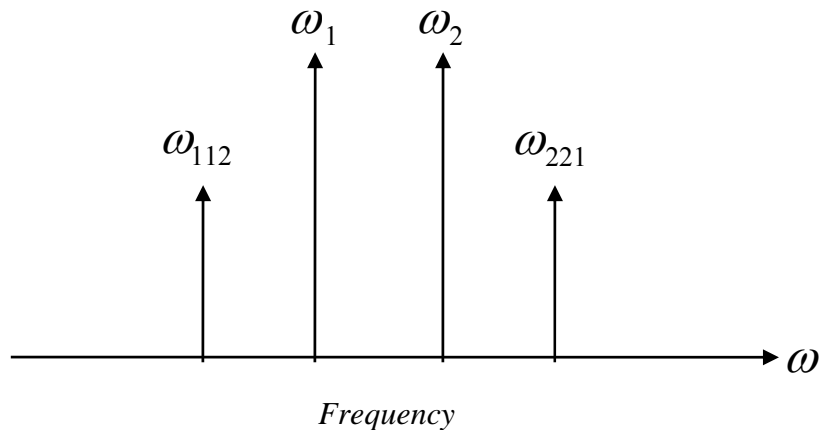


**Fig. 2.3 Additional frequencies generated through FWM**

If three unique frequencies are launched into fiber, there would be totally nine new frequencies generated, from the Equation (2.5.1). This effect is also called nondegenerate four-wave-mixing (Ref. [11]). Generally,  $N$  co-propagating wavelength in fiber could generate  $M$  additional frequencies through FWM, and their relationship is [3]:

$$M = \frac{1}{2}(N^3 - N^2) \quad (2.5.2)$$

The occurrence of FWM needs the condition of phase matching. That means, the efficiency of FWM depends on dispersion and channel spacing. Dispersion would lead to a group velocity mismatch, and furthermore destroy the phase matching condition. Therefore, high local dispersion fiber and larger channel spacing are beneficial in a WDM system.

## **3. Overview of Modulation Formats**

### **3.1. Introduction**

As we have said in Chapter 1, bit rate-distance product is a figure-of-merit of lightwave systems. To increase the capacity of lightwave systems, or bit rate-distance product, high speed data rate per channel and tighter channel spacing in DWDM systems are the possible solutions. 10Gb/s or 40Gb/s DWDM system would be the next generation of lightwave systems. In such high speed DWDM systems, linear and nonlinear impairments become severe. Those linear impairments include chromatic dispersion (CD), and first order polarization mode dispersion (PMD); nonlinear impairments include self-phase modulation (SPM), cross-phase modulation (XPM) and four-wave mixing (FWM).

To combat both the linear and the nonlinear impairments over the transmission fiber, an optimal modulation format is desired: A modulation format with narrow optical spectrum can enable closer channel spacing and tolerate more CD distortion; A modulation format with constant optical power can be less susceptible to SPM and XPM; A modulation format with multiple signal levels will be more efficient than binary signals and its longer symbol duration will reduce the distortion induced by CD and PMD. In addition, in an optical repetitive amplified lightwave system, amplified spontaneous emission (ASE) noise is another concern which requires modulation formats more tolerant to additive ASE noise.

There have been many optical modulation formats in the scope of this researching area. Because of its easy to modulate and demodulate, most of them are

binary signaling, e.g. duobinary, VSB/SSB, RZ, phase-shift-keying (PSK) etc.. While, others are multi-level signaling, e.g. differential-quadrature-phase-shift-keying (DQPSK), and M-PAM etc.. It is impossible to cover all of those modulation formats in this thesis. However, we will detail and compare several very important modulation formats often used in recent years. The modulation formats covered in this thesis are NRZ-OOK, RZ-OOK, CS-RZ, NRZ-DPSK and RZ-DPSK. Although this is not a complete screening of the advanced optical modulation formats arena, the results in this thesis and the mechanism under each modulation format are still valuable and can be extended for the future research.

In the following part, the basic waveform generation/detection and major characteristics of these five modulation formats will be discussed. It will form a foundation for the following parts of the thesis where system performance of different modulation formats will be detailed.

## **3.2. Generation and Characteristics of Several Modulation Formats**

### **3.2.1. NRZ-OOK**

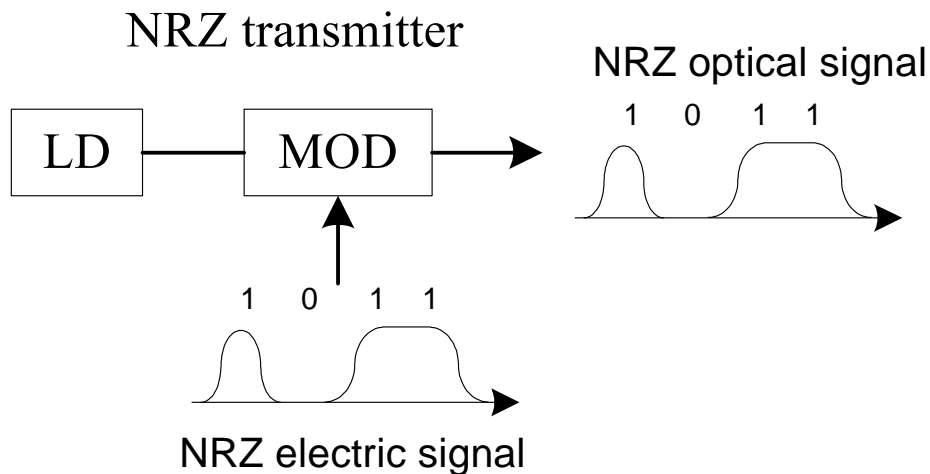
For a long time, non-return-to-zero on-off-keying (NRZ-OOK) has been the dominant modulation format in IM/DD fiber-optical communication systems. For convenience we would like to refer NRZ-OOK as NRZ. There are probably several reasons for using NRZ in the early days of fiber-optical communication: First, it requires a relatively low electrical bandwidth for the transmitters and receivers (compared to RZ); second, it is not sensitive to laser phase noise (compared to PSK); and last, it has the simplest configuration of transceivers. In recent years, as optical

communication is advancing to higher datarates, DWDM and long distance with optical amplifiers, NRZ modulation format may not be the best choice for high capacity optical systems. However, due to its simplicity, and its historic dominance, NRZ would be a good reference for the purpose of comparison.

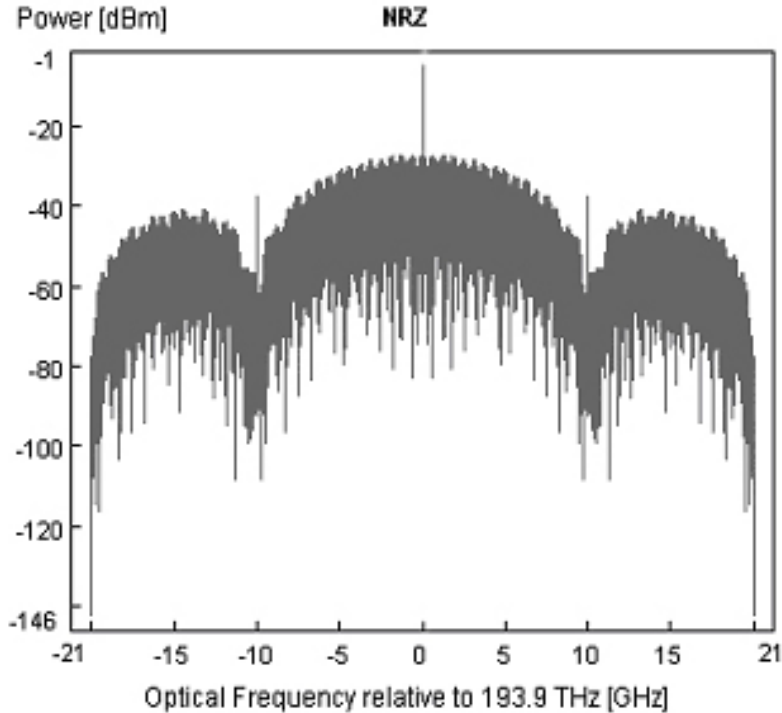
The block diagram of a NRZ transmitter is shown in Fig. 3.1, where electrical signal is modulated with an external intensity modulator. The intensity modulator can be either Mach-Zehnder type or electro-absorption type, which converts an OOK electrical signal with data rate of  $R_b$  into an OOK optical signal at the same data rate. The optical pulse width of each isolated digital “1” is equal to the inverse of the data-rate. To detect a NRZ optical signal, a simple photodiode is used at the receiver, which converts optical power of signal into electrical current. This is called direct detection (DD). If there is no mention, same direct detection scheme is used for other modulation formats.

Fig. 3.2 shows the spectrum of NRZ with 10Gbps of datarate. In general, NRZ modulated optical signal has the most compact spectrum compared to that with other modulate formats. However, this does not mean that NRZ optical signal has superior resistance to residual chromatic dispersion in an amplified fiber system with dispersion compensation. Also this does not mean NRZ is more tolerant to XPM and FWM in crowded DWDM systems because of its strong carrier component in the optical spectrum [13]. In addition, NRZ optical signal has been found to be less resistive to GVD-SPM effect in transmission compared to its RZ counterparts. A simple explanation is that different data patterns in a PRBS NRZ data stream require

different optimum residual dispersion for the best eye opening. For example, an isolated digital “1” would generate more self-phase modulation (SPM) effect than continuous digital “1”s. Since SPM can be treated as an equivalent signal frequency chirp, it modifies the optimum value of the dispersion compensation in the system. The difference in the optimum dispersion compensation between an isolated digital “1” and continuous digital “1”s makes it impossible to optimize the residual dispersion in the system and thus makes the system performance vulnerable to the data pattern-dependent fiber nonlinear effect. This effect is especially important in long distance fiber-optic systems.



**Fig. 3.1 Block diagrams of NRZ transmitter (Ref. [6])**



**Fig. 3.2 Optical spectrum of NRZ signal with 10 Gbps of data rate**

### **3.2.2. RZ-OOK**

RZ means ‘return-to-zero’, so the width of optical signal is smaller than its bit period. Usually a clock signal with the same data rate as electrical signal is used to generate RZ shape of optical signals. Fig. 3.3 shows the block diagram of a typical RZ transmitter. First, NRZ optical signal is generated by an external intensity modulator as we described in Chapter 3.2.1; Then, it is modulated by a synchronized pulse train with the same data rate as the electrical signal using another intensity modulator. RZ optical signal has been found to be more tolerant to nonlinearity than NRZ optical signal. The reason for its superior resistance to nonlinearity than NRZ is probably due to its regular data pattern of optical signal. Because of characteristic of

‘return-to-zero’ of RZ optical signals, an isolated digital bit ‘1’ and continuous digital “1”s would require the same amount of optimal dispersion compensation for the best eye opening. So with the optimal dispersion compensation in the system, RZ format shows better tolerance to nonlinearity than NRZ.

The spectrum of RZ is also shown in Fig. 3.4. Compared to NRZ, it has a wider spectrum because of its narrower pulse width. This would lead to less spectrum efficiency for RZ in a WDM system.

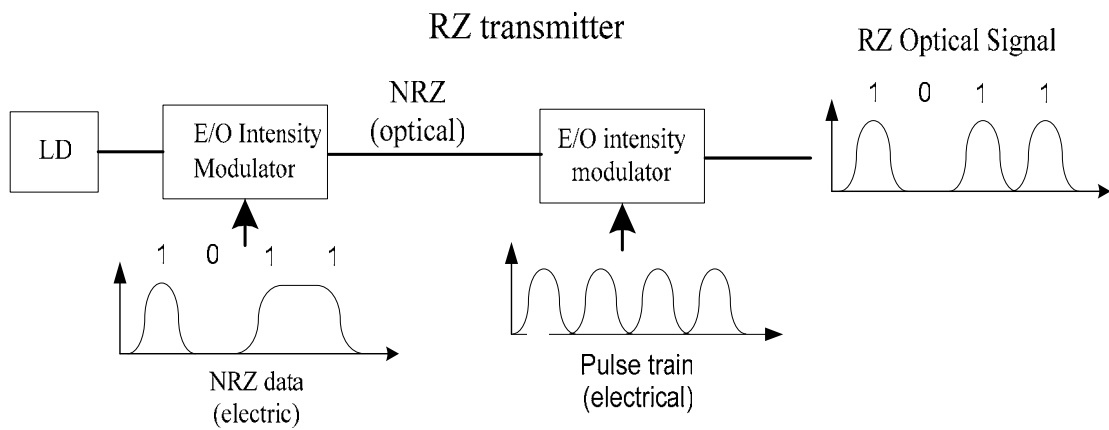


**Fig. 3.3 Block diagrams of RZ transmitter (Ref. [6])**

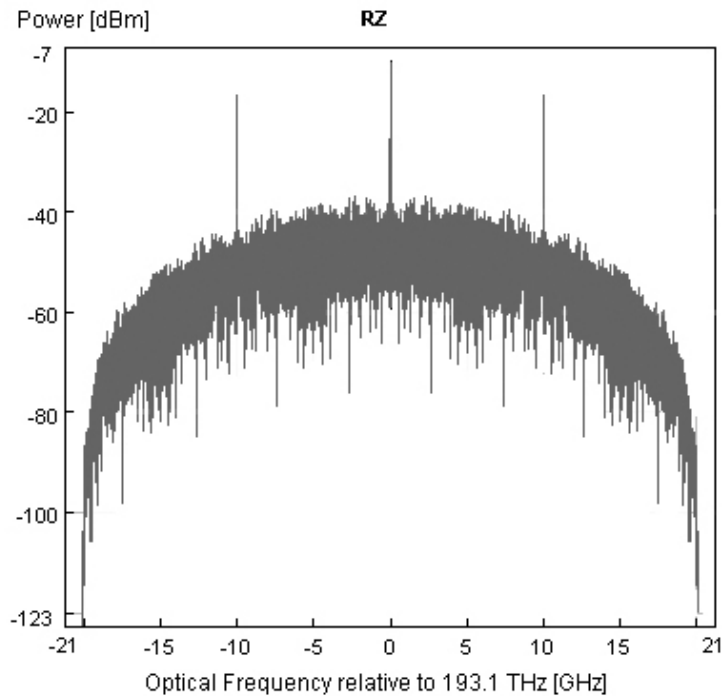


**Fig. 3.4 Optical spectrum of RZ signal with 10 Gbps of data rate**

### **3.2.3. NRZ-DPSK**

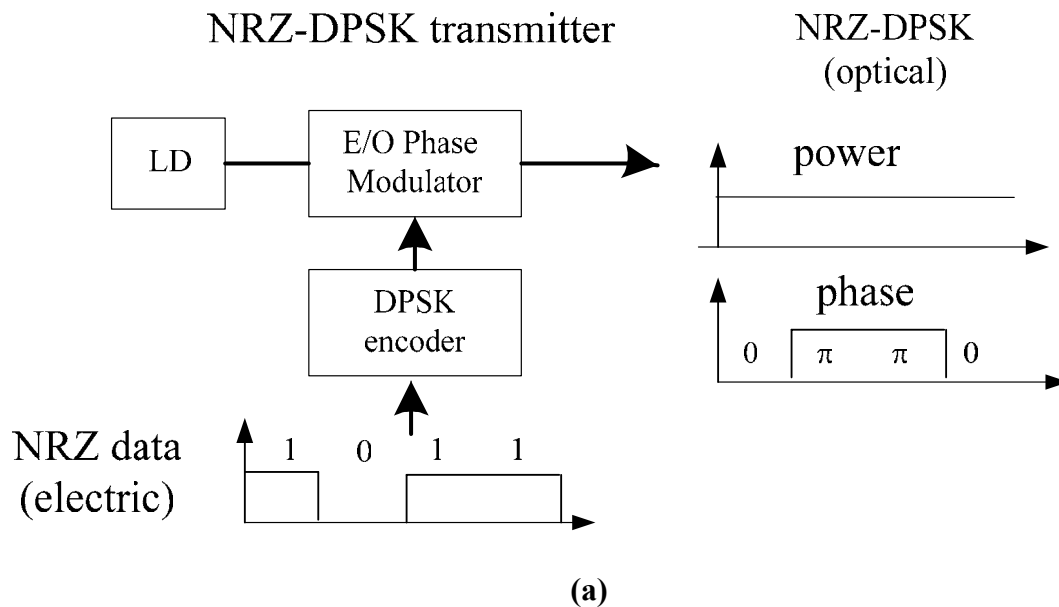
With optical intensity modulation, digital signal is represented by instantaneous optical power levels. Similarly, digital signal can also be represented by the phase of an optical carrier and this is commonly referred to as optical phase-shift-keying (PSK). In the early days of optical communications, because of the immaturity of semiconductor laser sources, the optical phase was not stable enough for phase-based modulation schemes. Recent rapid improvement of single-frequency laser sources and the application of active optical phase-locking make PSK feasible in practical optical systems. Specifically, differential-phase-shift-keying (DPSK) is the most often used format.

Fig. 3.5(a) shows the block diagram of a typical NRZ-DSPK transmitter. Before getting into the external phase modulator, NRZ electrical signal has to be pre-encoded by a DPSK encoder. In a DPSK encoder, the NRZ data is converted by a NOR gate first and then combined with its one-bit delay version by a XOR gate. This DPSK encoded electrical signal is then used to drive an electro-optic phase modulator to generate a DPSK optical signal. A digital “1” is represented by a  $\pi$  phase change between the consecutive data bits in the optical carrier, while there is no phase change between the consecutive data bits in the optical carrier for a digital “0”. A very important characteristic of NRZ-DPSK is that its signal optical power is always constant.

As shown in Fig. 3.5(b), a one-bit-delay Mach-Zehnder Interferometer (MZI) is usually used as a DPSK optical receiver. MZI is used to correlate each bit with its neighbor and make the phase-to-intensity conversion. There are two outputs of MZI, called constructive port or destructive port respectively. For constructive port, when the two consecutive bits are in-phase, they are added constructively in the MZI and results in a high signal level; otherwise, if there is a  $\pi$  phase difference between the two bits, they cancel each other in the MZI and results in a low signal level. For destructive port, it is vice-versa. In a practical DPSK receiver, both constructive port and destructive port of MZI are used, which is called balanced receiver. In a DPSK balanced receiver, a photodiode is used at each MZI output and then the two photocurrents are combined (logical subtract) to double the signal level. In this configuration, the receiver sensitivity is improved by 3dB compared to using only one

single photodiode in either constructive port or destructive port. At a certain input optical signal level, this means a 1.5dB increase in the receiver Q. In a DPSK system, since signal amplitude swings from “1” to “-1”, in the ideal case, when a balanced photo-detection and a matched optical filter are used, its receiver sensitivity is 3dB better than a conventional NRZ-OOK system, where the signal swings only from “0” to “1”.

For NRZ-DPSK coding, the optical power is constant. However, the optical field shifts between “1” and “-1” (or the phase shifts between “0” and “ $\pi$ ”) and the average optical field is zero. As a consequence, there is no carrier component in its optical spectrum as shown in Fig. 3.6. This differs from the spectrum of NRZ-OOK (Fig. 3.2), where the carrier component is strong.



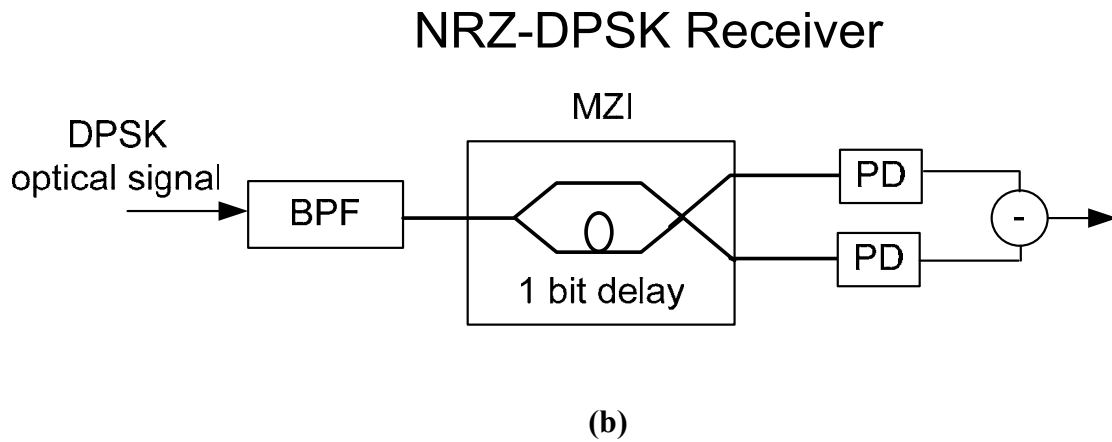


**Fig. 3.5** Block diagrams of NRZ-DPSK (a) transmitter and (b) receiver (Ref. [6])

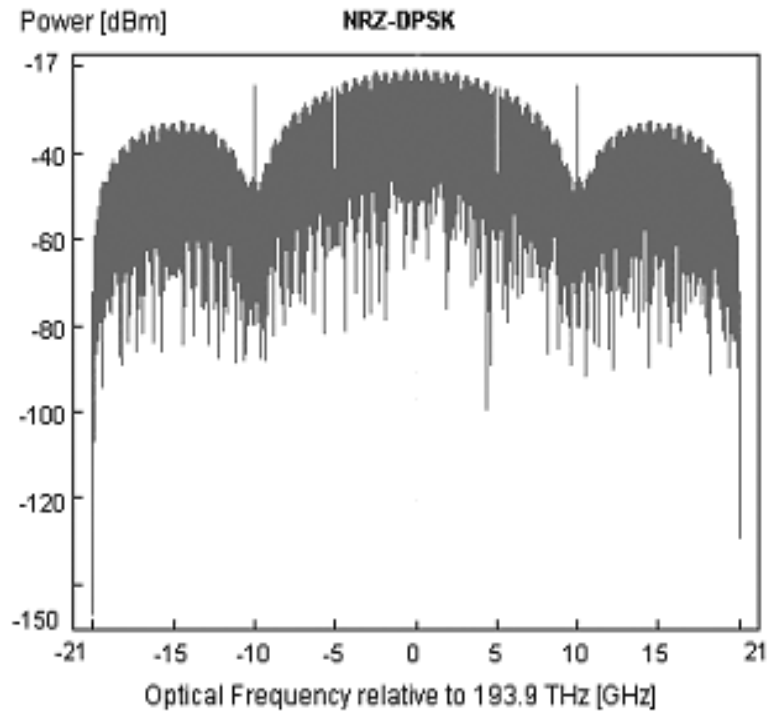


**Fig. 3.6** Optical spectrum of NRZ-DPSK signal with 10Gbps of datarate

Intuitively, because of its constant optical power the performance of NRZ-DPSK should not be affected by optical power modulation-related nonlinear effects

such as SPM and XPM. However, when the chromatic dispersion is considered, this conclusion is not entirely true. Phase modulations can be converted into intensity modulation through group velocity dispersion (GVD), and then SPM and XPM may contribute to waveform distortion to some extent [4]. In a long distance DPSK system with optical amplifiers, nonlinear phase noise is usually the limiting factor for phase-shift-keying optical signals. Several papers have proven that PSK or DPSK optical coding is vulnerable to nonlinear phase noise, a phenomenon called Gordon-mollenaur effect. Amplified spontaneous emission (ASE) noise generated by optical amplifiers is converted into phase noise through the Kerr effect nonlinearity in the transmission fiber; this disturbs the signal optical phase and causes waveform distortions.

#### **3.2.4. RZ-DPSK**

In order to improve system tolerance to nonlinear distortion and to achieve a longer transmission distance, return-to-zero DPSK (RZ-DPSK) has been proposed. Similar to NRZ-DPSK modulation format, the binary data encoded as either a “0” or a “ $\pi$ ” phase shift between adjacent bits. But the width of the optical pulses is narrower than the bit slot and therefore, the signal optical power returns to zero at the edge of each bit slot. In order to generate the RZ-DPSK optical signal, one more intensity modulator has to be used compared to the generation of NRZ-DPSK. The block diagram of a RZ-DPSK transmitter is shown in Fig.3.7. First, an electro-optic phase modulator generates a conventional NRZ-DPSK optical signal, and then, this

NRZ-DPSK optical signal is modulated by a clock signal with same datarate as the electrical signal through an electro-optic intensity modulator.

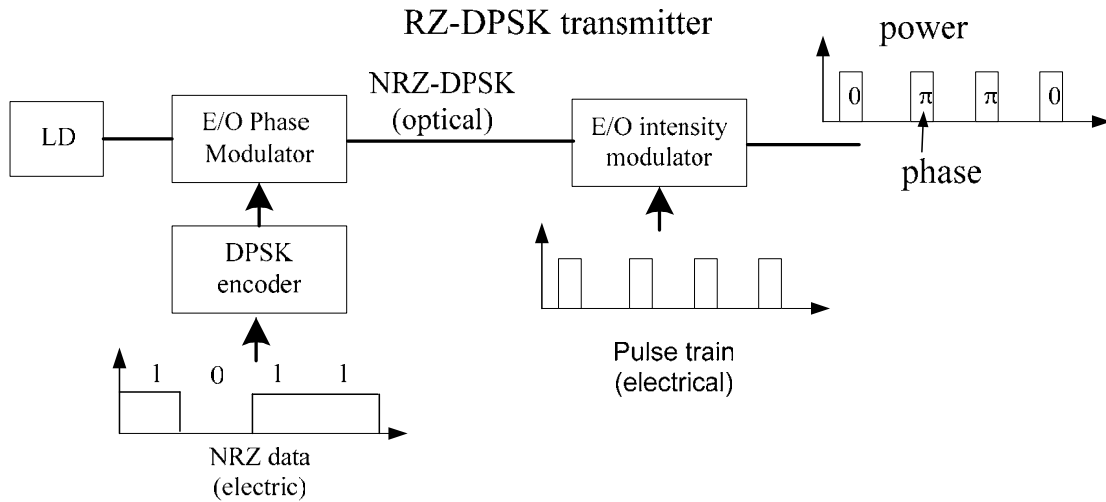


**Fig. 3.7** Block diagrams of RZ-DPSK transmitter (Ref. [6])

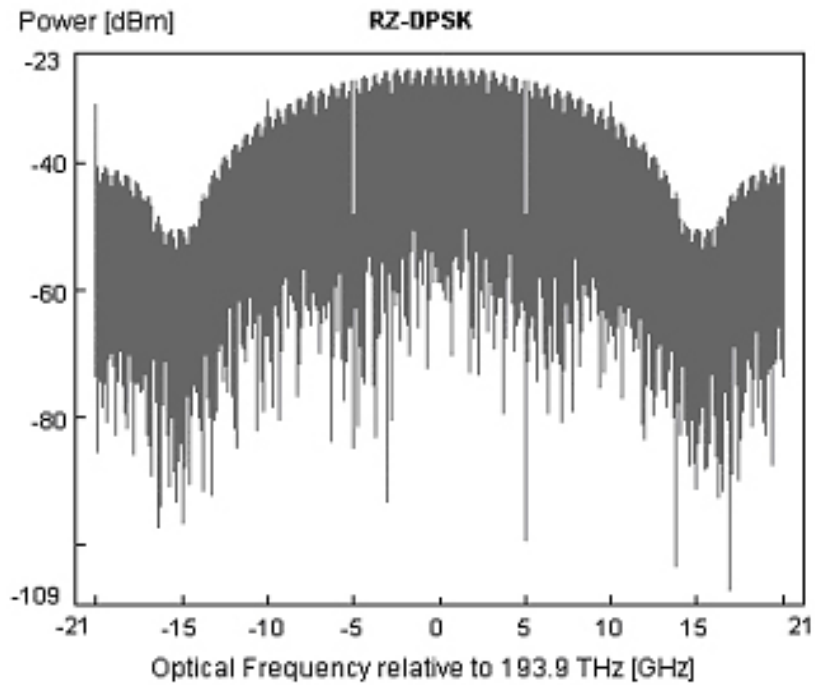


**Fig. 3.8** Optical spectrum of RZ-DPSK signal with 10Gbps of datarate

Sometimes RZ-DPSK is also referred to as intensity modulated DPSK (IM-DPSK) because of its additional bit-synchronized intensity modulation. In this modulation format, the signal optical power is no longer constant; this will probably introduce the sensitivity to power-related nonlinearity like SPM.

The spectrum of RZ-DPSK with 10Gbps of datarate is shown in Fig. 3.8. Due to the narrow optical signal pulse width, the optical spectrum of RZ-DPSK is wider than a conventional NRZ-DPSK. Intuitively, this wide optical spectrum would make the system more susceptible to chromatic dispersion. However, similar to RZ-OOK, RZ-DPSK is more tolerant to data-pattern dependent SPM-GVD effect with optimal dispersion compensation because of its regular RZ waveform.

### **3.2.5. CS-RZ**

Carrier-suppressed return-to-zero (CS-RZ) modulation format was proposed by Miyamoto in paper [5]. The major difference between a CS-RZ and a conventional RZ is that CS-RZ optical signal has a  $\pi$  phase shift between adjacent bits. Because of its phase alternation in the optical domain, there is no DC component for CS-RZ. As a consequence, there is no carrier component for CS-RZ in the spectrum as shown in Fig. 3.10. That is where the “carrier-suppression” comes from. Another characteristic for CS-RZ is that there are two clock components in its spectrum, which are half datarate away from the carrier.

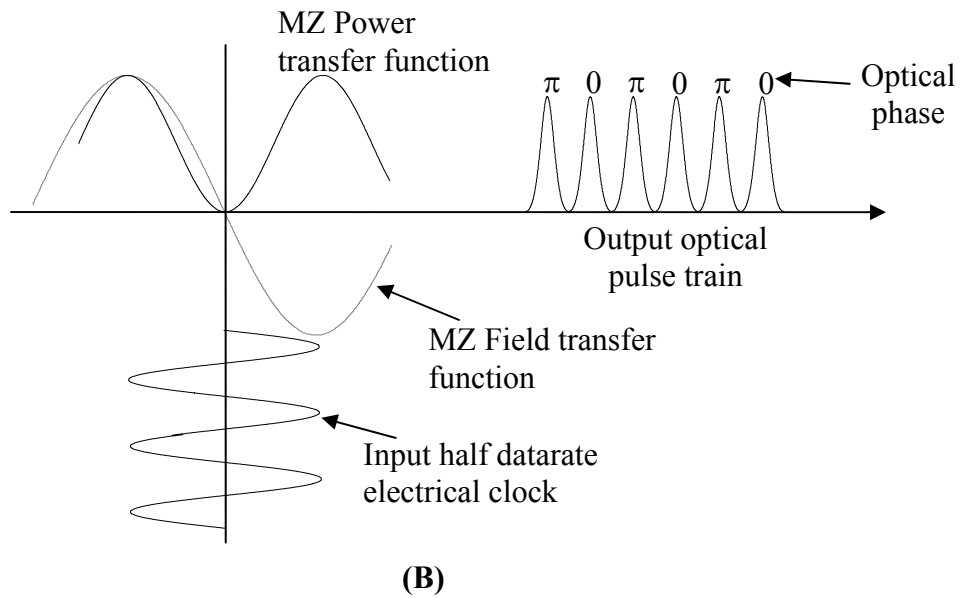
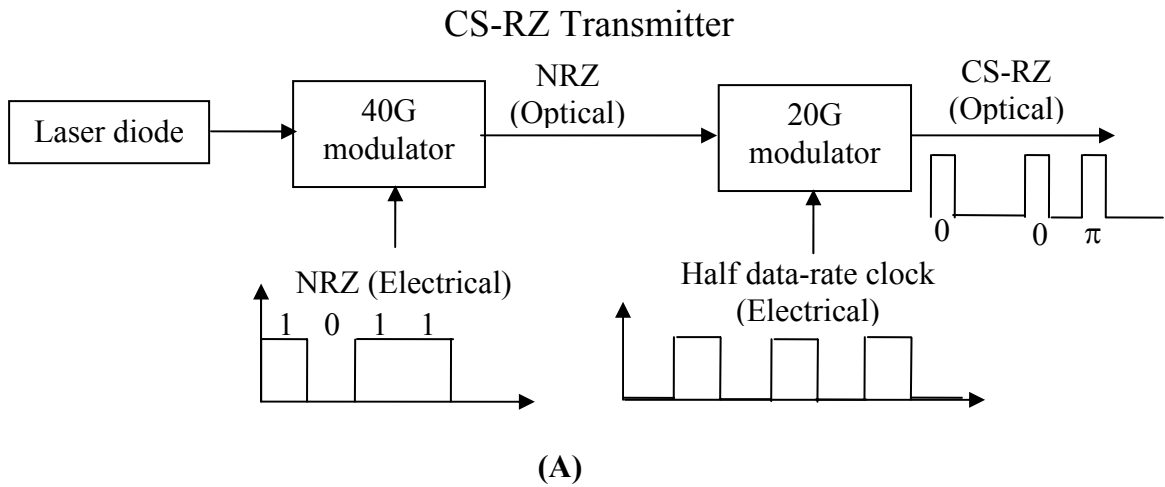


**Fig. 3.9 Block diagrams of CS-RZ transmitter and signal generation (Ref. [6])**

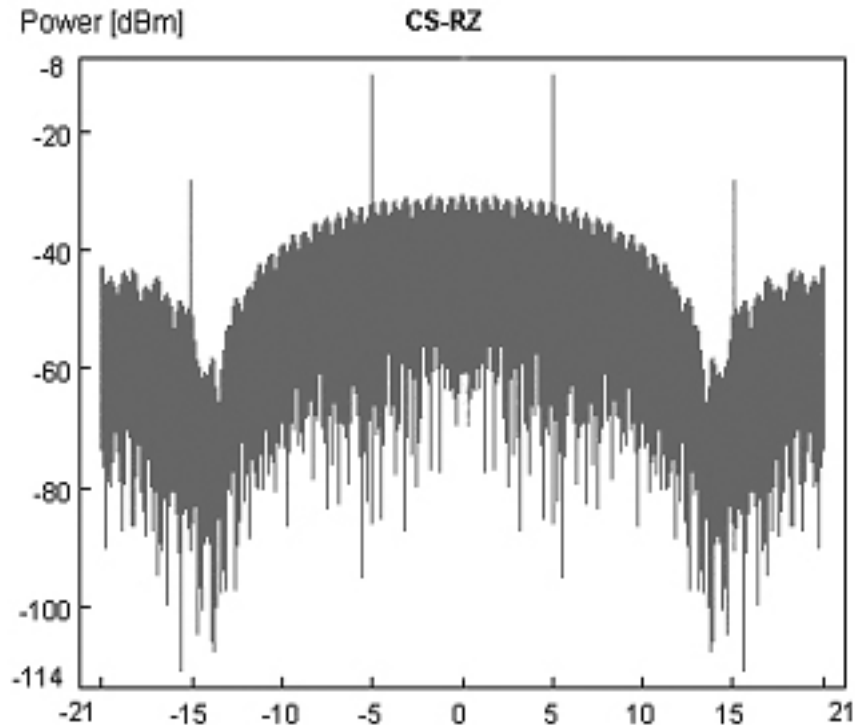


**Fig. 3.10 Optical spectrum of CS-RZ signal with 10 Gbps of datarate**

In general, the generation of a CS-RZ optical signal requires two electro-optic modulators as shown in Fig. 3.9 (A). In this configuration, the first intensity modulator encodes the NRZ data. Then the generated NRZ optical signal is modulated by the second intensity modulator to generate a CS-RZ optical signal. The second intensity modulator is biased at the minimum power transmission point and driven by a sinusoidal clock at the half datarate of the electrical signal. As illustrated in Fig. 3.9 (B), a MZ intensity modulator biased at this condition doubles the frequency of the modulating signal and the phase of output pulse train is alternated between '0' and ' $\pi$ '. This configuration only requires half datarate of bandwidth for the second electro-optical modulator, which reduces the complexity of configuration.

CS-RZ has shown better tolerance to fiber nonlinearity and residual chromatic dispersion in recent research [19]. Its RZ intensity bit pattern makes it easy to find the optimum dispersion compensation. In addition, carrier suppression reduces the efficiency of four wave-mixing in WDM systems.

## **4. Impact of Modulation Formats on Different Fibers**

### **4.1. Motivation**

With the development of lightwave technology, 10Gb/s and 40Gb/s optical systems are more and more increasing the attention of service providers. However dispersion and nonlinear degrading effects are becoming severe in such high speed optical systems. One of the key issues for the commercial realization of such high speed lightwave systems is to optimize the system performance through using optimum dispersion management and combating nonlinear degrading effects. On one hand, service providers just want to keep existing lightwave networks as much as possible. On the other hand, many factors like different fiber type and different modulation format could affect the system performance. Therefore, there is a need to compare various modulation formats on several possible fibers in the market. This would give us an insight view about the near future lightwave systems and assist the developing of our lightwave networks in a continuous way. In this Chapter, through comprehensive numerical simulations, we would compare the transmission performances of various advanced modulation formats on different types of optical fiber; and discuss their impact in the selection of transmission fiber types.

### **4.2. Schematic of System Setup**

The overall system configuration is shown in Fig.4.1. Both 40Gbps and 10Gbps data rate per wavelength are considered. The total system capacitor is assumed to be 1.6Tb/s. For 40Gb/s data-rate, 40 wavelength channels are used with the channel spacing of 100GHz (or equivalently 0.8nm). For 10Gb/s data-rate, we

have used 160 wavelength channels with 25GHz (0.2nm) channel spacing. Thus, the bandwidth efficiency is 25% for both cases. Simulations are performed in the C-band (1530nm – 1565nm).

Periodic optical amplifications are provided by inline erbium-doped fiber amplifier (EDFA) modules. Each EDFA module consists of a length of dispersion compensating fiber (DCF), which is sandwiched between two sections of erbium doped fibers and the noise figure of each EDFA is 4 dB. In-line EDFAs are used to 100% compensate the power loss over transmission fiber in each span. At the optical receiver, an optical pre-amplifier is used at each wavelength channel after the DEMUX to provide a +2dBm optical signal power for optical detection at the photodiode. Detailed system parameters are listed in Table 4.1, which includes the wavelength setting of channels, channel spacing, receiver optical bandwidth (channel bandwidth in optical DEMUX), and receiver electrical bandwidth.

For the purpose of comparison and identification of degradation sources, we have also calculated the performances of systems with single wavelength. The single-wavelength carrier is set as 193.9THz, corresponding to the middle channel in WDM systems, which is Channel No.20 in 40 GHz system or Channel No.80 in 10 GHz system. No optical MUX and DEMUX are used in the single carrier systems. Instead, a bandpass optical filter centered at 193.9 THz is used in the receiver with the same characteristics as the DEMUX in WDM systems (Table 4.1) and there is no optical filter used in the transmitter.

There are four different types of fibers used in the simulations. They are Standard Single Mode Fiber (SMF), True Wave fiber (TW), True Wave-Reduced Slope fiber (TW-RS) and Large Effective Area Fiber (LEAF). Table 4.2 lists the major physical parameters of these fibers. The parameters of dispersion compensation fiber (DCF) are also listed in Table 4.2. To make a fair comparison between these fibers, we require perfect dispersion slope compensation for all of them in the simulation. That means except for a different dispersion slope of DCF used with each different transmission fiber, other DCF parameters are assumed to be identical when used in different transmission fiber systems. It is not difficult to find the required dispersion slope of DCF  $S_{DCF}$  to make a perfect dispersion slope compensation in different fiber systems:

$$S_{DCF} = S_{fiber} \times \frac{D_{DCF}}{D_{fiber}} \quad (4.1.1)$$

where  $S_{fiber}$  and  $D_{fiber}$  are the Dispersion Slope and Dispersion parameters (Table 4.2) for different kinds of transmission fibers.  $D_{DCF}$  is the Dispersion parameter of the DCF in different transmission fiber systems.

In the system a dispersion pre-compensation module is inserted immediately after the WDM multiplexer. For each different modulation format at each power level and each fiber type, the single-channel transmission performance is optimized by adjusting the value of pre-compensation from  $-1000$  ps/nm to  $0$  ps/nm. Then this optimum value of pre-compensation is used in the corresponding WDM scenario (the

multi-channel system using the same modulation format, same fiber types and same power level per channel as the single channel case).

In WDM systems simulation, the overall residual dispersion of central wavelength channel at frequency of 193.9THz is set to be zero through adjusting the length of DCFs in the transmission line. The feature of dispersion map of central channel in the simulation is illustrated in Fig. 4.2, where dispersion compensation is distributed evenly in each span. For channels other than the central channel, we adjust the value of the tunable dispersion compensator at each wavelength after DEMUX to compensate for the residual dispersion at that wavelength. Both the MUX at the transmitter and the DEMUX at the receiver were considered as ideal ones without insertion loss.

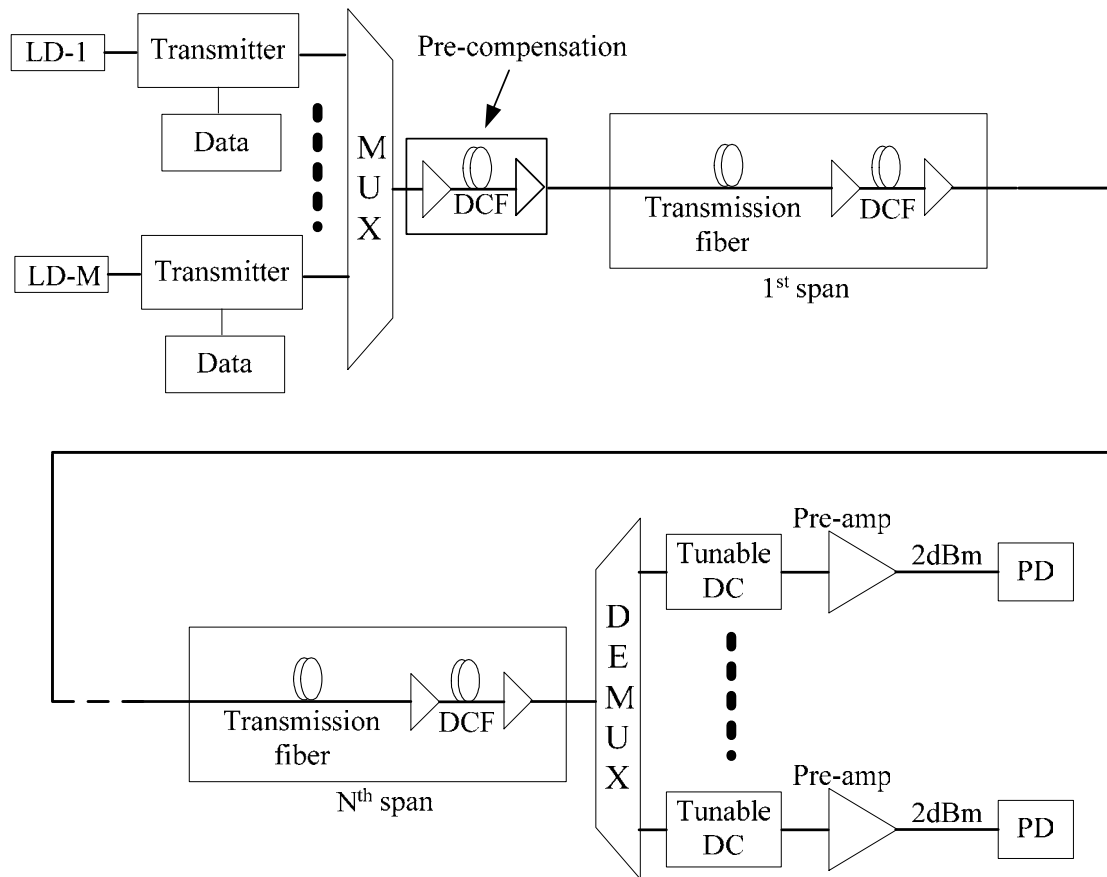


**Fig. 4.1 Schematic of WDM system setup (Ref. [6])**

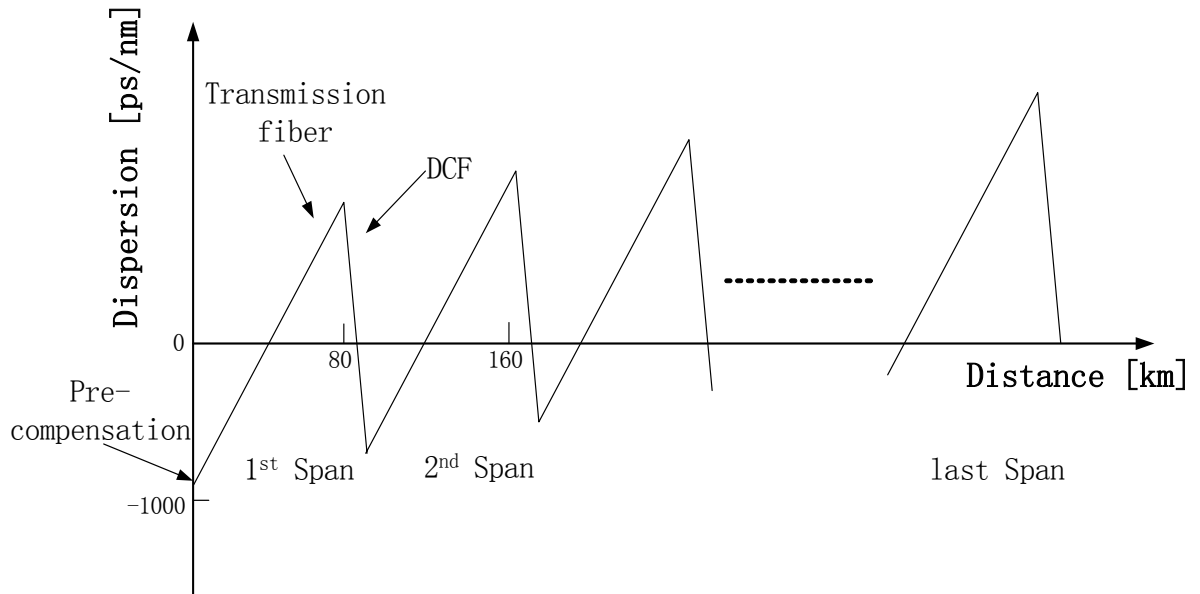


**Fig. 4.2 Dispersion management in simulation**

**Table 4.1: System Parameters (Ref. [6])**

	<b>10 GHz system</b>	<b>40 GHz system</b>
Number of channels	160	40
Channel wavelengths	Ch1 ... Ch80 ... Ch160 1563.1nm...1547.2nm...1531.4nm	Ch1 ... Ch20 ... Ch40 1562.5nm...1547.2nm...1531.4nm
Channel spacing	25 GHz	100 GHz
Total capacity	1.6 Tb/s	1.6 Tb/s
Optical filter in DEMUX	20 GHz Bessel filter, 6 <sup>th</sup> order	80 GHz Bessel filter, 6 <sup>th</sup> order
Bandwidth of LPF in receiver	7 GHz Bessel filter, 6 <sup>th</sup> order	28 GHz Bessel filter, 6 <sup>th</sup> order
Length of trans. fiber per span	80 km	80 km
Number of spans	5, 10, 15, 20	5, 10, 15, 20
Dispersion Management	100% dispersion compensated ideal dispersion slope compensated	100% dispersion compensated ideal dispersion slope compensated
Output power of preamplifier	+2 dBm per channel	+2 dBm per channel
NF of EDFA [dB]	4	4

**Table 4.2: Physical Parameters of all kinds of Fiber (Ref. [6])**

	Dispersion D @ 1550nm [ps/nm/km]	Dispersion slope S @1550nm [ps/nm <sup>2</sup> /km]	Nonlinear refractive index $n_2$ [10 <sup>-20</sup> m <sup>2</sup> /W]	Effective core area $A_{eff}$ [μm <sup>2</sup> ]	Fiber attenuation $\alpha$ [dB/km]
Standard SMF	17	0.058	2.8	80	0.25
DCF for SSMF	-90	$0.058 \times \frac{-90}{17}$	4.3	14.3	0
TW	3.5	0.08	3.45	45	0.25
DCF for TW	-90	$0.08 \times \frac{-90}{3.5}$	4.3	14.3	0
TW-RS	4.4	0.045	3.2	55	0.25
DCF for TW-RS	-90	$0.045 \times \frac{-90}{4.4}$	3.0	14.3	0
LEAF	3.7706	0.11	3.0	72	0.25
DCF for LEAF	-90	$0.11 \times \frac{-90}{3.7706}$	4.3	14.3	0

### 4.3. Computer Simulation Model

A commercial simulation package “VPI transmission maker” is used in this work. There also a number of assumptions in the simulations: (1) the rise and fall time of the electrical data signals is one quarter of the data period. (2) the electro-optic intensity modulator is chirp-free. (3)  $2^7-1$  PRBS with 512 bits is used as the data pattern (4) the input power of DCF is controlled less than  $-27\text{dBm/ch}$  to make the nonlinearity induced by DCF negligible (5) no forward error correction (FEC) is used. The basic mechanism behind the simulator is to solve the nonlinear Schrödinger equation using the split-step Fourier Transformation. In order to calculate the Q value

at the receiver, the accumulated ASE noise from optical amplifiers are combined analytically with the eye opening in the waveform by

$$Q = \frac{\mu_1 - \mu_0}{\sigma_1 + \sigma_0} \quad (4.2.1)$$

Where  $\mu_1$  and  $\mu_0$  are average signal levels at logical “1”s and “0”s respectively, and  $\sigma_1$  and  $\sigma_0$  are noise standard deviations for at logical “1”s and “0”s.

In WDM optical systems, because of the nonlinear crosstalk, the middle channel generally has the worst performance. Therefore, in our simulations, the Q factor of the middle channel (Ch20 in the 40 GHz system or Ch80 in the 10 GHz system) is measured in all cases. Also, since Q equal to 6 when the BER (bit error rate) is  $10^{-9}$  without FEC, we will use Q of 6 as the criteria in comparisons later.

#### **4.4. Simulation Results**

There are totally four kinds of modulation formats considered in the simulation: NRZ, CS-RZ, NRZ-DPSK, and RZ-DPSK. Please refer to Chapter3.2 for their characteristics and generations/detections. Based on the system described above, we have done a series of computer simulations to compare these four optical modulation formats and their performance over different fiber types. Both 40 Gb/s and 10 Gb/s systems are investigated in the simulation. In addition to presenting the results of WDM optical systems, performances of systems with single channel are also presented for comparison. The presentation of simulation results and discussion are grouped into 40 Gb/s and 10 Gb/s systems.

#### 4.4.1 40 Gb/s Optical systems

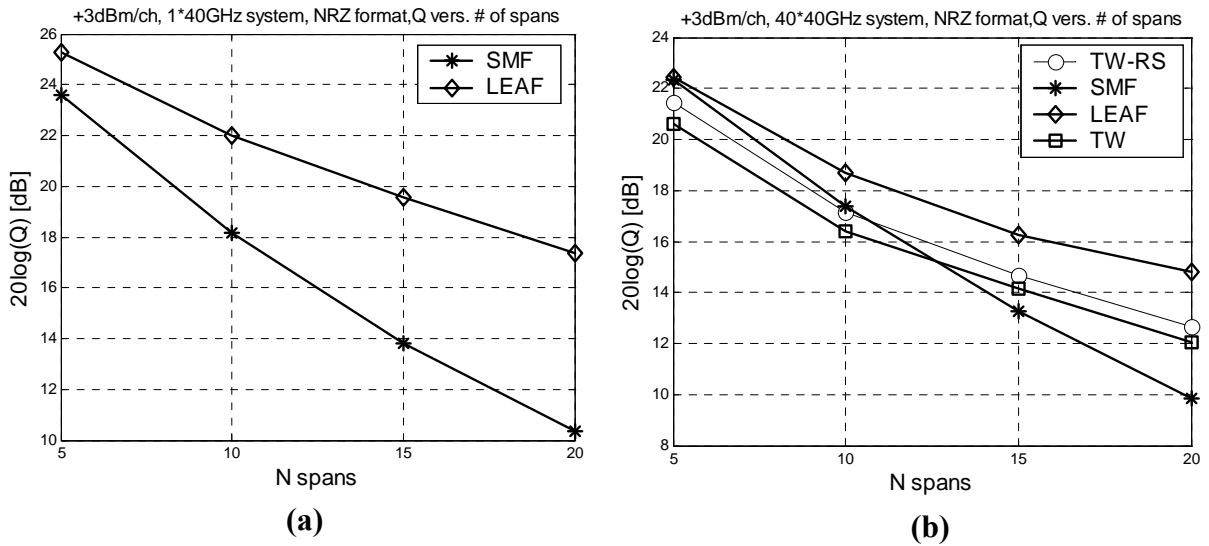
The simulated system  $Q$  factor versus the number of fiber spans for 40Gb/s data rate are presented in this section and shown from Fig. 4.3 to Fig.4.6.

Fig.4.3 shows the system performance using NRZ modulation format. Fig. 4.3(a) compares single-wavelength transmission performance between SMF-28 and LEAF. It is obvious from this figure that LEAF fiber performs better than SMF-28 and that this superiority becomes more significant with increasing number of spans. Since this is only a single channel in the system and no nonlinear crosstalk is involved, the only degradation is attributed to SPM nonlinearity.

Fig. 4.3(b) shows the simulated result for NRZ in a 40 Gb/s per channel and 40 channel WDM system. In addition to SPM, nonlinear cross-talks such as XPM and FWM are now also involved. Comparing Fig. 4.3(a) with Fig. 4.3(b), it is evident that the  $Q$ -value for the system using LEAF fiber is decreased significantly because of the nonlinear crosstalk while there is only a small degradation in the  $Q$ -value for the system using SMF-28. The high local dispersion of SMF-28 created a strong walk-off between WDM channels during transmission and it minimizes the nonlinear crosstalk between them. In this particular system, however, SMF-28 still provides the lowest  $Q$ -value after 15 spans of transmission among all four fiber types. The low nonlinear crosstalk penalty due to a high local dispersion in SMF-28 does not offset the high SPM penalty in a DWDM application.

It is worth to point out that the fiber related performance strongly depends on the chosen optical signal modulation format. Fig. 4.4(a) shows an example of the

system performance using a carrier-suppressed return-to-zero (CS-RZ) modulation format on both SMF-28 and LEAF fibers in single channel 40 Gb/s system. Comparing Fig. 4.4(a) with Fig. 4.3(a) it is evident that the performance difference between SMF-28 and LEAF is smaller by using CS-RZ. This is attributed to the improved dispersion tolerance of CS-RZ which reduces the penalty due to SPM. Similarly, Fig. 4.4(b) shows the simulated result of a 40 channel WDM system with 40 Gb/s datarate per channel. All the four fiber types were tested here for comparison. Although LEAF still provides the best performance at long transmission distances, the difference between LEAF and SMF-28 is very small.



**Fig. 4.3 NRZ in 40 GHz systems, 3dBm per-channel average power (Ref. [6]) (a) Single Channel and (b) 40-λ WDM with 100GHz channel spacing**

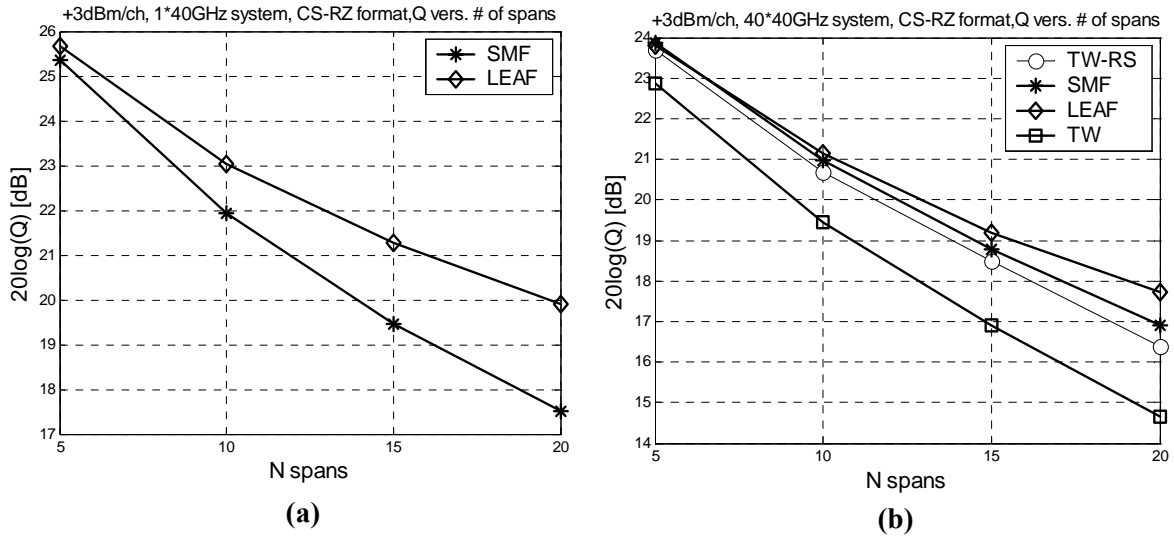


**Fig. 4.4 CS-RZ in 40 GHz systems, 3dBm per-channel average power (Ref. [6]) (a) Single Channel and (b) 40- $\lambda$  WDM with 100GHz channel spacing**

Fig. 4.3 and Fig. 4.4 demonstrate that in 40Gb/s optical systems, SPM is one of the major contributors for system performance degradation. Especially for SMF-28, which has the highest local chromatic dispersion, the effect of SPM is the strongest. It is noticed that both NRZ and CSRZ are intensity modulation-based optical systems and SPM is originated from the signal intensity modulation. Intuitively, optical phase modulation-based lightwave systems would significantly reduce the effect of SPM because the optical power is not modulated.

Fig. 4.5 shows the system performance using NRZ-DPSK modulation. Fig.4.5(a), compares single-wavelength transmission performance between SMF-28 and LEAF. In this case, there is almost no performance difference between SMF-28 and LEAF in this single-channel system. This is easy to understand: because NRZ-DPSK has the constant optical power, so the SPM is not significant here. Fig. 4.5(b) shows the simulation result for NRZ-DPSK in the WDM scenario, where nonlinear

cross-talks such as XPM and FWM are involved. Nonlinear crosstalks introduce strong performance degradation in fiber systems with low chromatic dispersions, while the Q value reduction for the system with SMF-28 is not significant. The high local dispersion of SMF-28 creates a strong walk-off between WDM channels during transmission and it minimizes the nonlinear crosstalk between them. Fig. 4.5(b) clearly demonstrate that in a 40Gb/s multi-channel WDM optical system with 100GHz channel spacing, SMF-28 has the best performance among all fiber types when NRZ-DPSK modulation is used. In this case, the optimum optical power level per channel is 0dBm.

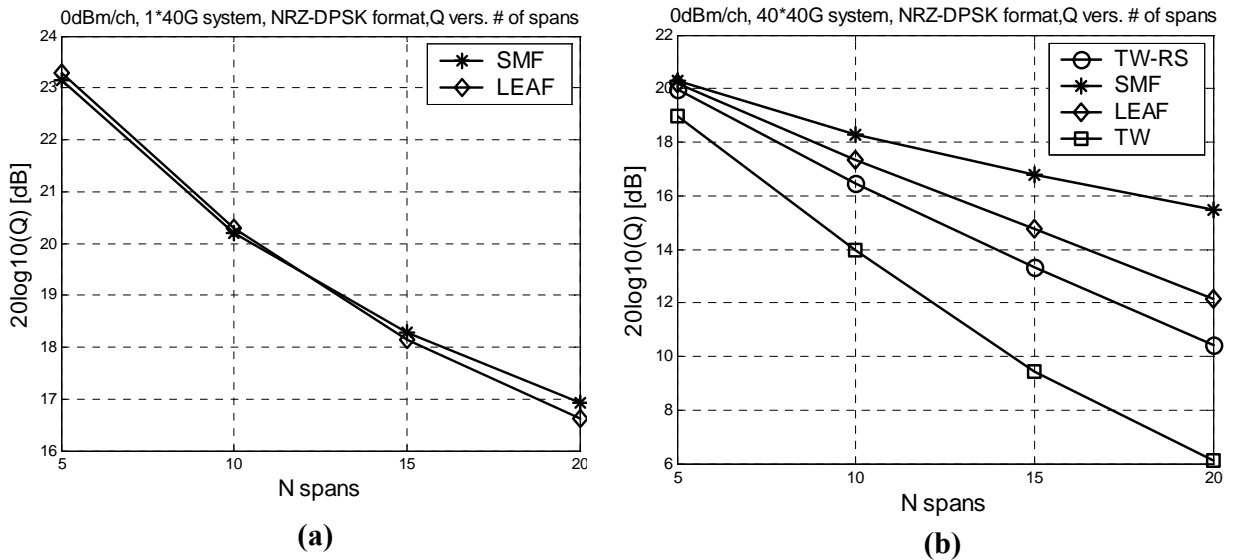


**Fig. 4.5 NRZ-DPSK in 40 Gb/s systems, 0dBm per-channel average power (Ref. [6])**  
**(a) Single Channel and (b) 40-λ WDM with 100GHz channel spacing**

Another modulation format we have investigated is RZ-DPSK. Fig.4.6 summarizes the simulation results for this modulation format. Once again, Fig. 4.6(a) compares single-wavelength transmission performance between SMF-28 and LEAF.

Because of the added intensity modulation in RZ-DPSK systems, the effect of SPM cannot be neglected. Therefore, LEAF performs better than SMF-28 in this single channel case. However, compared to other intensity modulation formats, the performance difference between LEAF and SMF-28 is less significant with RZ-DPSK and there is only an approximately 1.5dB difference in the receiver Q value at the 20<sup>th</sup> span. When multi-channel WDM is considered as shown in Fig. 4.6(b), the performance difference between SMF-28 and LEAF becomes negligible. Stronger nonlinear crosstalk in low local dispersion fibers, such as LEAF, in DWDM applications offsets the strong SPM penalty in high local dispersion fibers such as SMF-28. It is interesting to note that using this modulation format, all fiber types have similar performance except for the poor performance of the TW fiber. This is because the nonlinear parameter  $\gamma$  for the TW fiber is particularly high.

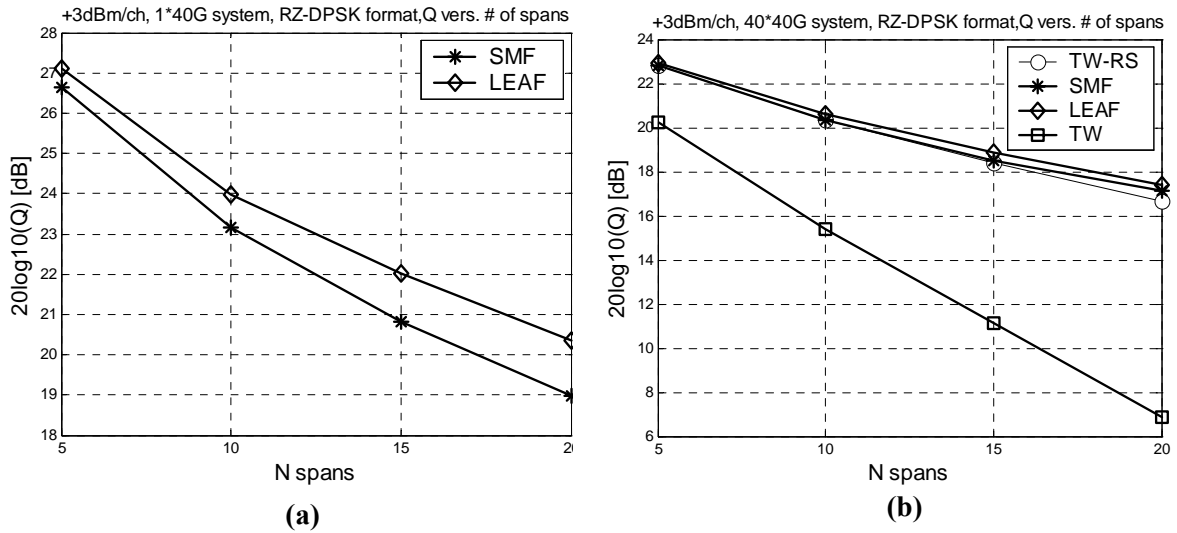


**Fig. 4.6 RZ-DPSK in 40 GHz systems, 0dBm per-channel average power (Ref. [6]) (a) Single Channel and (b) 40- $\lambda$  WDM with 100GHz channel spacing**

To summarize, for 40Gb/s optical systems with intensity modulation, SPM is one of the most important sources of performance degradation. For high local dispersion fibers such as SMF-28, the effect of SPM is stronger than low local dispersion fibers such as LEAF and TW-RS [15]. On the other hand, SMF-28 has lower sensitivity to nonlinear crosstalk in WDM systems because of the rapid walk-off between adjacent wavelength channels [17]. When optical phase modulation is applied, such as NRZ-DPSK, SPM is not a big concern. In this case SMF-28 outperforms other types of fibers in WDM systems.

Overall, however, the best performance for a transmission distance of 1,600km (20 spans) was obtained by using RZ-DPSK. With this modulation format, SMF-28, LEAF and TW-RS fibers have similar performances. If there is some way to

compensate for the effect of SPM, SMF-28 would become the best choice of the fiber type.

#### **4.4.2 10 Gb/s Optical Systems**

Sine the effect of SPM is proportional to the square of the signal datarate, the SPM effect in 10Gb/s system would be 16 times less than that in 40Gb/s system. Therefore, the performance comparison of different modulation formats over different fibers in 10Gb/s system will differ from what we get in 40Gb/s above. We have also performed computer simulations in 10Gb/s datarate DWDM systems, which have a narrower channel spacing (25GHz) and 160 multiplexing wavelengths to assure the same bandwidth efficiency and capacity as the 40Gb/s systems.

The results of 10 Gb/s system are presented in the plots from Fig 4.7 to Fig 4.8. The optical power levels per wavelength used in the simulation is -3dBm for all the different modulation formats to achieve the best performances. At this signal optical power level, we have confirmed that SPM is not the major degrading effect in 10Gb/s systems. Fig. 4.7 compares the Q-values between the SMF-28 and the LEAF fiber systems for a single-channel transmission using four different modulation formats.

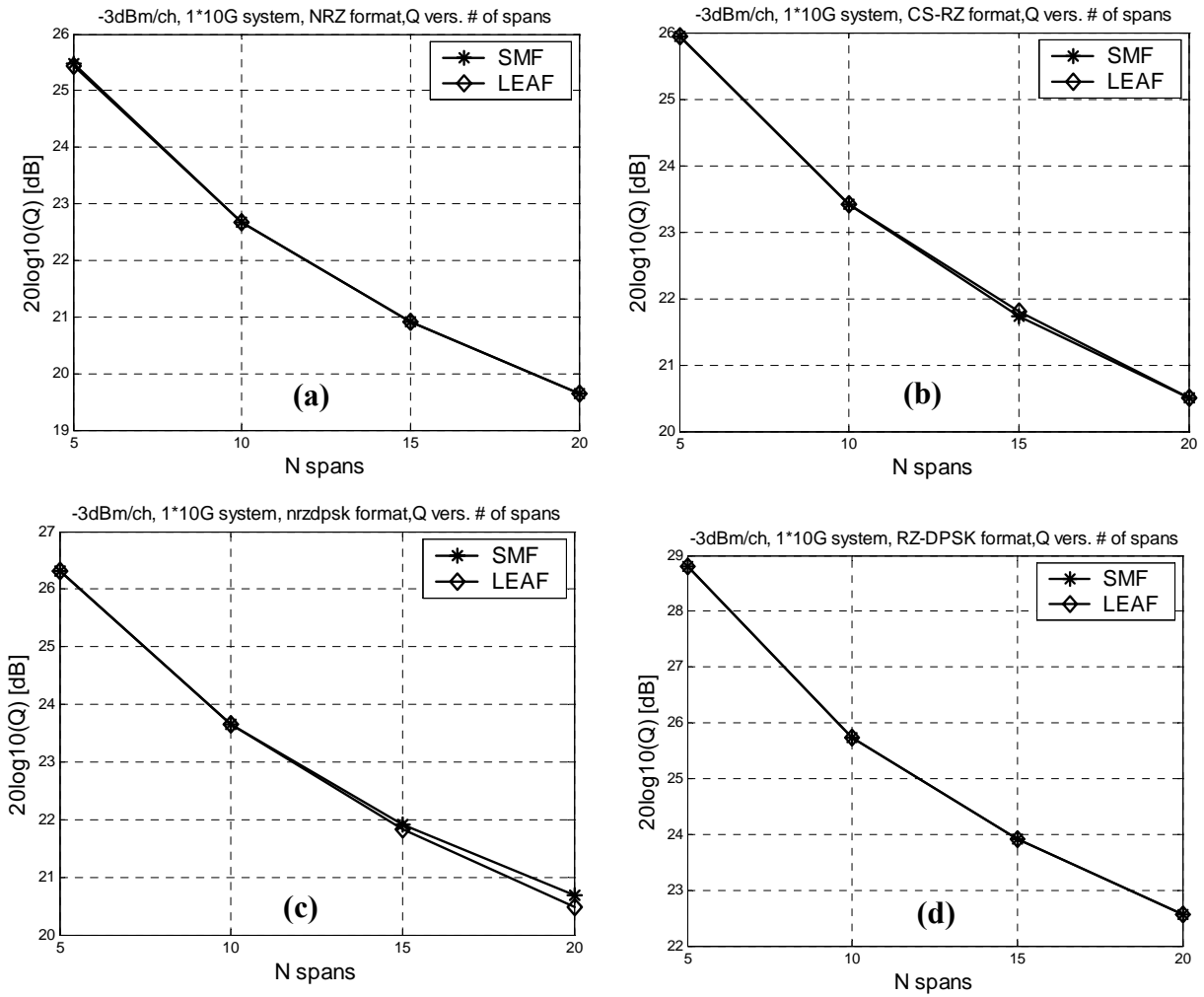


**Fig. 4.7 Comparison between SMF-28 and LEAF fibers in a single channel 10 GHz system, -3dBm per-channel average power. (a) NRZ , (b) CS-RZ, (c) NRZ-DPSK and (d) RZ-DPSK (Ref. [6])**

Fig. 4.7 shows that for single wavelength operation at 10Gb/s data-rate, SMF-28 and LEAF fibers have almost identical performances for all the four different optical modulation formats. In this case, the receiver Q value reduction at larger number of spans is mainly due to the accumulated ASE noise of the optical amplifiers. Fig. 4.7 clearly proves that the effect of SPM is not significant in a 10Gb/s system at

this power level. For WDM systems, on the other hand, nonlinear crosstalk will have to be considered.

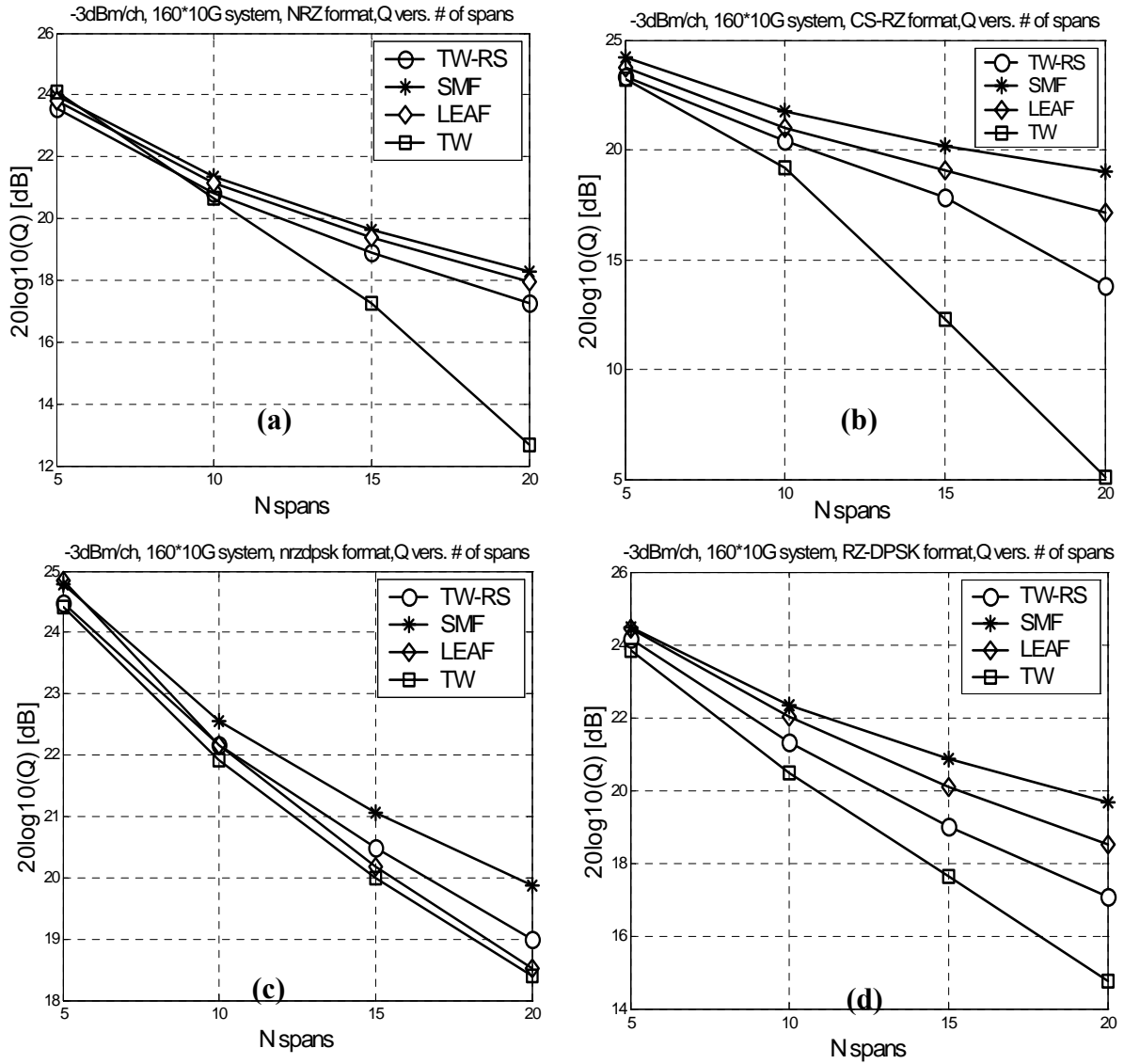


**Fig. 4.8** 160- $\lambda$ , 10Gb/s systems with 25GHz channel spacing and -3dBm per-channel average power: (a) NRZ, (b) CS-RZ, (c) NRZ-DPSK and (d) RZ-DPSK (Ref. [6])

Fig.4.8 shows the simulated Q values for 10Gb/s DWDM systems with 160-wavelength, 25GHz channel spacing and -3dBm average signal optical power per

channel. All the four optical modulation formats were investigated each operating with different fiber types. It is not surprising that SMF-28 always has the best performance because of its high local dispersion and thus high resistance to nonlinear crosstalk compared to other types of fibers with low local dispersion.

By comparing results in Fig.4.8 for 10Gb/s systems with those for 40Gb/s systems shown in Fig.4.3 through Fig. 4.6, it is quite clear that at 20 fiber spans, the performance of 10Gb/s systems are always better than that of the 40Gb/s systems although they have the same optical spectral efficiency. In addition, SMF-28 has clear competitive advantages for relatively low data rate DWDM systems with narrow channel spacing.

## **4.5 Conclusion**

So far, we have investigated the performance of 10Gb/s and 40Gb/s optical systems with various optical modulation formats and various types of fibers, which is summarized in Table 4.3. For 10Gb/s DWDM systems with narrow channel spacing, nonlinear crosstalk originated from XPM and FWM are major sources of system performance degradation. No matter what optical modulation format is used, standard single-mode fiber (SMF-28) always has the best performance compared to other types of fibers. This is due to the high local dispersion of SMF-28, which creates a strong walk-off between different wavelength channels and reduces the effect of nonlinear crosstalk. On the other hand, for 40Gb/s optical systems with 100GHz channel spacing, SPM was identified as the major source of performance degradation if NRZ modulation format was used. SPM effect can be reduced to some extent by using

advanced modulation formats and optical phase modulation provides the optimum suppression to SPM effect because no intensity modulation is involved. Since SPM effect is strong in fibers with high local dispersion, how to effectively reduce the effect of SPM will be a key for practical application of 40Gb/s optical transmission in SMF-28 based fiber plants.

**Table 4.3: Summary of comparison between different formats over different fibers**

	<b>40Gbps × 1ch</b>	<b>40Gbps × 40ch</b>	<b>10Gbps × 1ch</b>	<b>10Gbps × 160ch</b>
NRZ	LEAF>SSMF	LEAF is best	LEAF=SSMF	SSMF is best
CS-RZ	LEAF>SSMF	LEAF is best	LEAF=SSMF	SSMF is best
NRZ-DPSK	LEAF=SSMF	SSMF is best	LEAF=SSMF	SSMF is best
RZ-DPSK	LEAF>SSMF	LEAF≈SSMF≈ TW-RS, TW is worst	LEAF=SSMF	SSMF is best

SPM is a parasitic phase modulation caused by signal optical power modulation and fiber nonlinearity, which broadens the signal optical spectrum. In intensity modulated, direct detection systems, this parasitic phase modulation and spectral broadening will not cause performance degradation by itself. This parasitic phase modulation, however, can be converted into an unwanted intensity modulation through chromatic dispersion of the transmission fiber, thus causing waveform distortion. From this point of view, high chromatic dispersion makes a system particularly vulnerable to SPM. Although dispersion compensation at the end of each fiber span can correct for the waveform distortion caused by linear chromatic

dispersion, it cannot completely compensate for the distortion caused by SPM. The major reason is that SPM-induced parasitic phase shift is created along the fiber in a continuous way and the SPM created at each location requires a different value of optical dispersion compensation. This problem becomes more significant when the signal data rate is high and the dispersion length is comparable to the effective nonlinear length. Here, the dispersion length is defined by  $L_D = 2\pi c T^2 / (\lambda^2 D)$  and the effective nonlinear length is defined by  $L_{eff} \approx 1/\alpha$ , where  $T$  is the signaling time period,  $D$  is the dispersion parameter and  $\alpha$  is the fiber attenuation parameter. For SSMF, the attenuation is 0.2 dB/km ( $\alpha \approx 0.0461[\text{Neper}/\text{km}]$ ) and  $D = 17[\text{ps} \cdot \text{nm}^{-1} \cdot \text{km}^{-1}]$ . The effective nonlinear length is then  $L_{eff} \approx 22\text{km}$ . For a 10 Gb/s bit-rate, the dispersion length is  $L_D = 462\text{km}$ , which is much longer than the nonlinear length, while for a 40Gb/s bit-rate, the dispersion length is approximately  $L_D = 29\text{km}$ , which is now similar to the nonlinear length. Since SPM is created continuously within the fiber nonlinear length and dispersion-induced pulse broadening is significant during this fiber length for 40Gb/s transmission, waveform distortion caused by SPM is expected to be significant, even with optimum dispersion compensation.

The effect of SPM can be mitigated by using phase modulation based optical transmission such as NRZ-DPSK. In fact, SMF-28 has the best performance among all fiber types using this modulation format. However, NRZ-DPSK does not necessarily provides the best performance overall compared to other modulation

formats and using other fiber types. It would be very useful if we can find a method to actively compensate for the effect of SPM. It is well known that there are other nonlinear degrading factors like XPM and FWM except SPM in a real WDM system. But like we have demonstrated above, in 40Gb/s systems with 100GHz of channel spacing, SPM is one of the most degrading factor and it is still helpful to find a way to compensate for SPM alone. This could be another researching direction extended from this simulation.

## 5. Impact of Modulation Formats on Dispersion-managed Optical Systems – A Simplified Model

### 5.1. Motivation

As we have demonstrated in Chapter 4, SPM is one of the major nonlinear degrading effects in high speed datarate (e.g. 40Gb/s) WDM systems. In addition, the modulation format is a key issue to combat SPM, e.g. in Chapter 4, NRZ-DPSK format is found to be the most tolerant to SPM and saves SMF-28 fiber as an optimal fiber concerning the single SPM effect. Then next question is how to find a way to combat SPM degrading effect. Nonlinear Schrödinger Equation has confined the way how optical waveform evolved over fibers and how SPM interferes with the waveform. Solving Nonlinear Schrödinger Equation would be the direct way to our question. Unfortunately, it is hard to find a simple and complete resolution for the Schrödinger equation. Numerical simulation becomes a good way to measure the degrading effects due to SPM and further find some way to combat SPM nonlinear effect. The drawback of numerical simulation which uses split-step method mostly is that it is time-consuming. So is there some way to simplify the numerical simulation model concerning SPM degrading effect in lightwave systems?

In this chapter, we would devote to find the simple relationship between signal optical power  $P$  and SPM-limited transmission distance  $L_{SPM}$ , a simplified model. Also several modulation formats are investigated and they are non-return-to-zero (NRZ), return-to-zero (RZ), carrier-suppressed return-to-zero (CS-RZ) and return-to-zero differential-phase-shift-keying (RZ-DPSK). How this simplified model

helps on comparing the system performance of four modulation formats and designing a lightwave system will be shown.

## 5.2. System Setup and Numerical Model

The block diagram of the basic system setup used for simulation is shown in Fig. 5.1. Systems of both 10Gb/s and 40Gb/s are evaluated with the same system setup. This is a single-channel optical system at the wavelength of 1547 nm. At the transmitter, a binary electrical data stream is converted into a different modulated optical signal and a  $2^6-1$  PRBS data pattern is used to drive the modulator in the simulation. Four possible modulation formats used in the transmitter are NRZ, RZ, CS-RZ or RZ-DPSK; please refer to chapter 3 for the generation of these four formats and their detection. A simple PIN photodiode is used in the receiver for direct-detection of NRZ, RZ and CS-RZ optical signals, while a Mach-Zehnder Interferometer (one-bit differential optical delay line) and balanced receiver is adopted in the RZ-DPSK optical receiver (Chapter 3). An EDFA post amplifier is used in the transmitter to boost the optical signal into a desired power level. There are totally  $N$  amplified transmission fiber spans in the simulation. Each fiber span, except the last one, consists of 100 km of standard single mode fiber (SSMF) and a dispersion compensating fiber (DCF) module. In the inline span, the DCF module has 21.25 km of DCF sandwiched between two inline-EDFAs. The noise figure of each EDFA is 4 dB. The characteristics of both SSMF and DCF are summarized in Table 5.1.

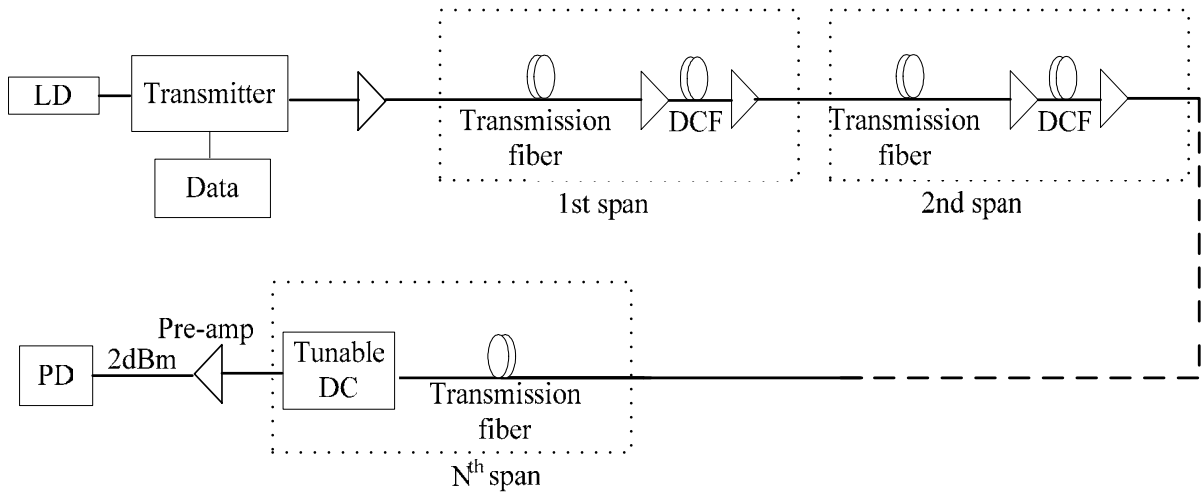


**Fig. 5.1 Block Diagram of System Setup**

**Table 5.1: Fiber parameters in the simulation**

	SSMF	DCF
Dispersion parameter $D$ [ $s/m^2$ ]	$17e-6$	$-80e-6$
Nonlinear index $n_2$ [ $m^2/W$ ]	$2.43e-20$	$4.3e-20$
Core area $A_{eff}$ SSMF [ $m^2$ ]	$72e-12$	$14.3e-12$
Attenuation $\alpha$ [dB/km]	0.2	0.5

The nonlinear effect due to DCF is negligible by setting the output power of the first EDFA less than  $-20$ dBm. The total optical loss over SSMF and DCF in each inline span is 100% compensated by two inline-EDFAs. A band-limiting optical filter with the bandwidth of  $B_o = 2B$  is used in the simulation and the electrical bandwidth of the receiver is set to be  $B_e = 0.65B$ , where  $B$  is the signal datarate. The dispersion map in the simulation is shown in Fig. 5.2. The length of the DCF (21.25 km) is chosen to completely compensate the chromatic dispersion of the SSMF of each span,

except for the last span ( $N^{\text{th}}$  span) where the length of DCF is varied in each simulation to optimize the signal eye-opening.

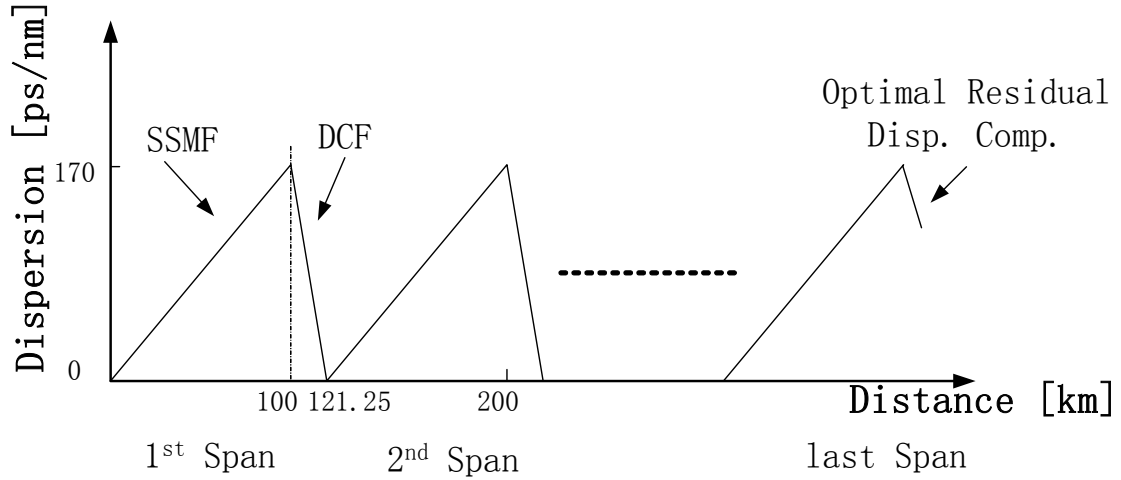


**Fig. 5.2 Dispersion management in the simulation**

To exclude the ASE noise influence from the SPM-induced nonlinear distortion, ASE noise is turned off in all the numerical simulations. At each input optical signal power level, for different modulation format, a maximum transmission distance is found, which is defined as the distance at which the eye-opening-penalty (EOP) reaches 1dB. We call this distance as SPM-limit on transmission distance  $L_{\text{SPM}}$ . Fig. 5.3 just shows an example how we calculate the  $L_{\text{SPM}}$  in simulations. In Fig. 5.3, eye-opening-penalty (EOP) along the transmission distance (including both SSMF and DCF) is calculated, when average input power of 12dBm and NRZ optical coding are used in the simulation. It is obvious to see that there is a two-peak structure in the plot of Fig. 5.3. Each of two peaks of EOP occurs at the end of SSMF and DCF in each span respectively. When optical signal is input into the SSMF of each span with desired optical power, because of chromatic dispersion and

nonlinearity over SSFM, its waveform is distorted and the EOP increases gradually. When optical signal reaches the end of SSMF, its EOP reaches the first peak in each span. Then, EOP is brought down because of dispersion compensation by DCF. When optical signal arrives at the optimal length of DCF, its EOP is the smallest in each span. After that, EOP of optical signal increases again because of over dispersion compensation, and it reaches its second peak in each span. Even with optimal dispersion compensation, the nonlinear SPM effect could not be fully compensated, thus the minimum EOP with the optimal dispersion compensation in the last span in Fig. 5.3 will increase gradually as the number of span increases. Maximum number of spans  $N_{\max}$  is then found when the EOP with the optimal dispersion compensation is less than or equal to 1 dB. Thus, Maximum transmission distance induced by SPM effect  $L_{\text{SPM}}$  is defined as the product of  $N_{\max}$  and the length of SSMF in each span (100 km).

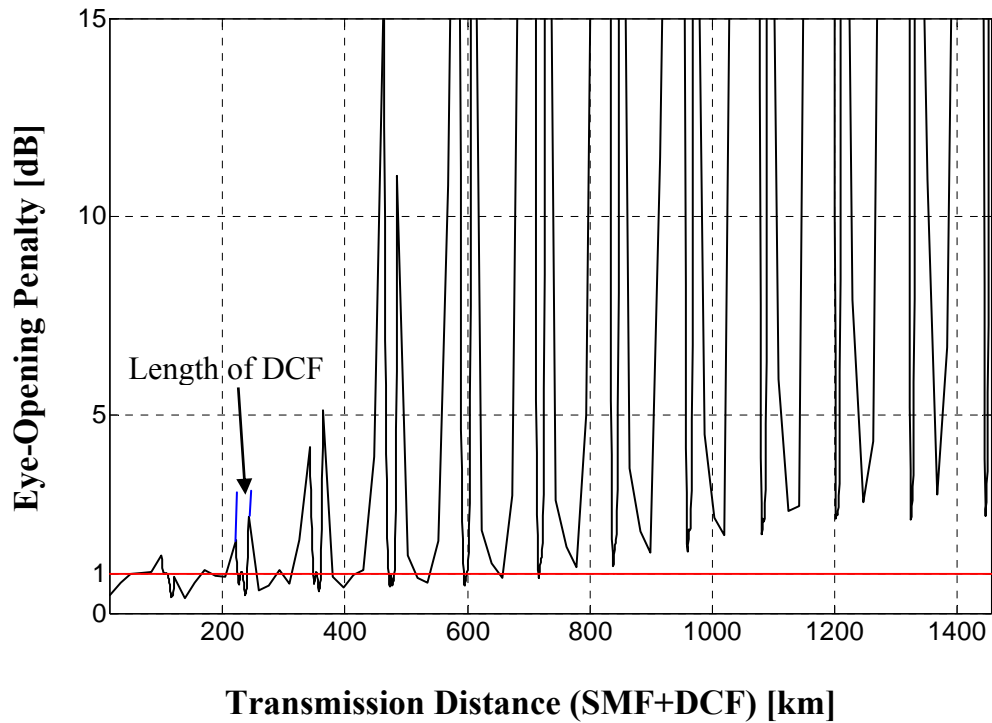


**Fig. 5.3 EOP of signal evolves over the transmission distance, with 12dBm average input power and NRZ format**

### 5.3. Simulation Results and Discussion

Fig.5.4 shows the calculated maximum SPM-limited transmission distance versus the average signal optical power at the input of each transmission fiber span in 10Gb/s system. Scattered points in Fig.5.4 represent numerically simulated maximum SPM-limited transmission distance with NRZ (diamonds), RZ (squares), CS-RZ (stars) and RZ-DPSK (circles) modulation formats. A remarkable feature of this plot is that for all modulation formats investigated, transmission distance  $L_{SPM}$  in logarithm scale is inverse-proportional to the average signal optical power in dBm. Such linear relationship can be expressed as:

$$L_{SPM} \cdot P = C \quad (5.3.1)$$

where  $C$  is a constant depending on signal modulation formats, and  $L_{SPM}$  is in unit of Meter and average input power  $P$  is in unit of Watt. Solid lines in Fig. 5.4 are the curve fittings using Equation (5.3.1). The difference between investigated modulation formats is just the constant  $C$ -value.

Similarly, Fig. 5.5 shows the maximum SPM-limited transmission distance versus the average signal optical power at the input of each transmission fiber span in 40Gb/s system. Not surprisingly, the same linear relationship for all modulation formats holds in 40Gb/s system though SPM degrading effect is much larger than its counterpart 10Gb/s system. Also, using Equation (5.3.1), we can get the similar curve fittings in 40Gb/s system.

Table 5.2 shows the  $C$ -value of curve fittings for various modulation formats in both 10Gb/s and 40Gb/s systems. At 10Gb/s datarate as shown in Fig. 5.4, there is no obvious difference between various modulation formats and their  $C$ -values differ by less than 20% as shown in Table 5.2. This indicates that in low datarate dispersion-managed optical systems, SPM-induced limitation is relatively insensitive to the signal modulation formats. This is attributed to the fact that at low datarate, the dispersion length is much longer than the nonlinear length of the fiber for all the modulation formats discussed here. On the other hand, at 40Gb/s as shown in Fig. 5.5, system tolerance to SPM-induced nonlinear distortion is strongly affected by signal modulation formats. For example, the  $C$ -value for RZ-DPSK is approximately 400% larger than the  $C$ -value for NRZ. At this datarate, the dispersion length becomes

comparable or even shorter than the nonlinear length of the fiber depending on the signal modulation formats and the signal modulation format plays an increasingly important role in determining the resistance against the nonlinear degradation such as SPM. This result is consistent with the studies in paper [4] and [8].

**Table 5.2: Power-  $L_{SPM}$  product  $C$  for different modulation formats in  $[mW \cdot km]$  (Ref [7])**

Data-rate	NRZ	RZ	CS-RZ	RZ-DPSK
10 Gb/s	11222	10294	12926	9254
40 Gb/s	855	1683	2864	3636

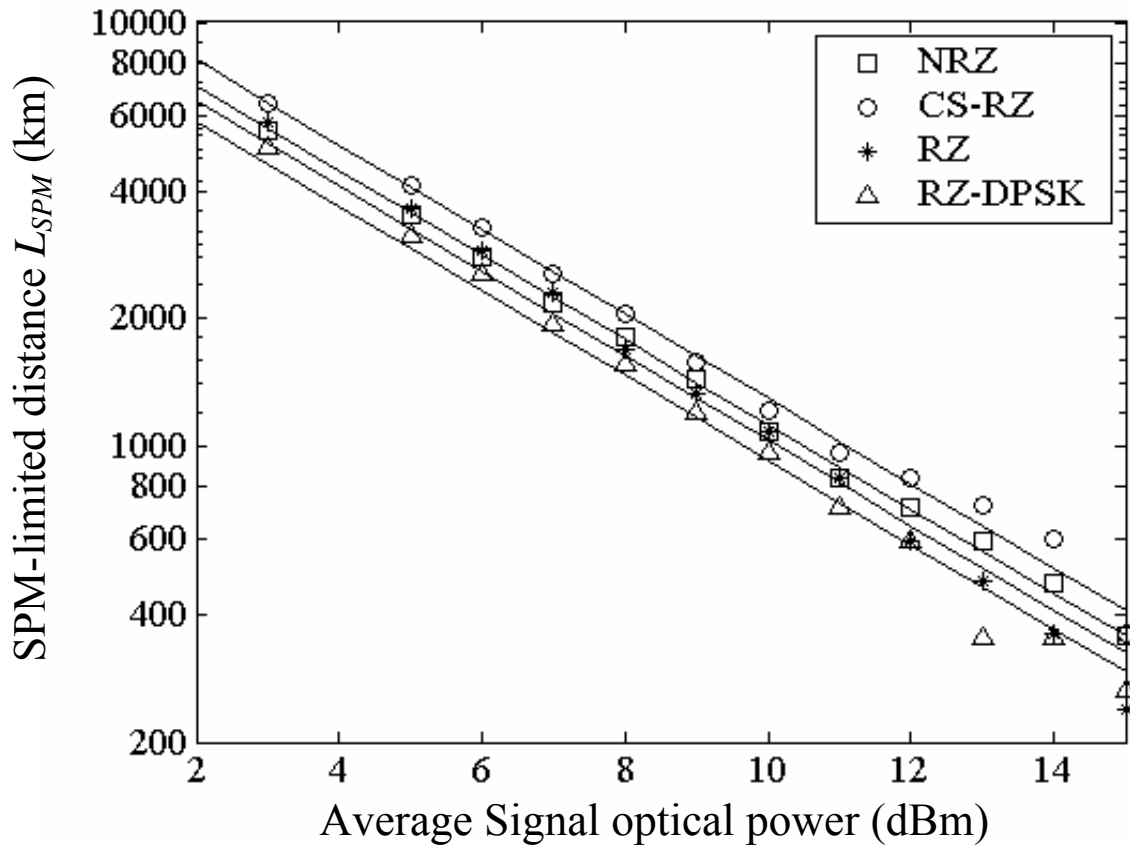
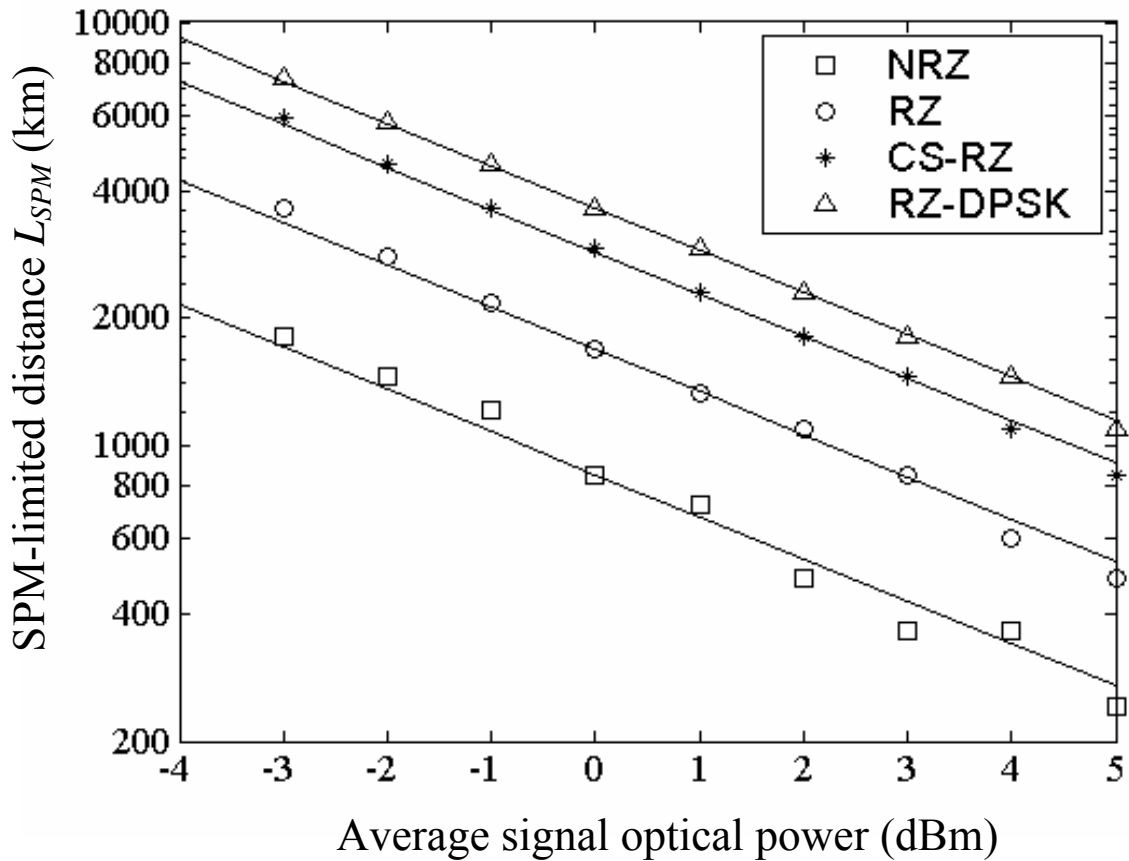


Fig. 5.4 SPM-limited transmission distance versus launched optical power for 10Gb/s data rate. Scattered points: results of numerical simulations. Solid lines: linear fittings between  $\log(L_{SPM})$  and  $P(\text{dBm})$  with the slope of  $-1$ .



**Fig. 5.5 SPM-limited transmission distance versus launched optical power for 40Gb/s data rate. Scattered points: results of numerical simulations. Solid lines: linear fittings between  $\log(L_{SPM})$  and  $P(\text{dBm})$  with the slope of  $-1$ .**

#### 5.4. Impact of ASE Noise

Above numerical simulations discussed in Chapter 5.3 reveals that the simple relationship between SPM-limited transmission distance and signal optical power, as indicated by Equation (5.3.1), is valid for various optical modulation formats and RZ-DPSK is the most tolerant to SPM-induced waveform distortion at high datarate. In practical optical systems, another major limitation to the transmission distance is the

accumulated ASE noise generated by inline EDFAs through the degradation of receiver SNR. Neglecting signal waveform distortion and considering the action of signal-spontaneous beat noise alone in the receiver, SNR-limited receiver  $Q$ -value is directly proportional to the square-root of optical signal power [1, 14, 15],

$$Q = \sqrt{\frac{\lambda \cdot P_{in}^{(1)}}{2 \cdot N \cdot h \cdot c \cdot NF_{eff} \cdot (G_{eff} - 1) \cdot B_e}} \quad (5.4.1)$$

Where  $P_{in}^{(1)}$  is the optical power of bit “1” launched into each fiber span,  $h$  is the Planck’s constant,  $c$  is the speed of light,  $\lambda$  is the signal wavelength,  $B_e$  is the receiver bandwidth and  $N$  is the total number of amplified fiber spans. In this noise calculation, each DCF module, which consists of a dispersion compensating fiber sandwiched between two in-line EDFAs, is considered as an equivalent optical amplifier with the effective noise figure  $NF_{eff} = 4.4\text{dB}$  and the effective optical gain  $G_{eff} = 20\text{dB}$ , which compensates for the loss of 100km transmission fiber. Using Equation (5.4.1) and setting  $Q = 10$ , we have calculated SNR-limited transmission distance for NRZ, RZ, CS-RZ and RZ-DPSK in both 10Gb/s and 40Gb/s systems, which are shown as dashed straight lines in Fig. 5.6 (for 10Gb/s system), and in Fig. 5.7 (for 40Gb/s system). In both Fig. 5.6 and Fig. 5.7, RZ and CS-RZ are identical and they perform better than NRZ because of the higher peak power. RZ-DPSK has the best SNR performance because of its bipolar nature of the signal and using of a balanced receiver.

However, it is well known that DPSK modulation might be vulnerable to the Gordon-Mollenauer effect [12, 16, 17] where ASE optical intensity noise can be

converted into phase noise through fiber nonlinearity. When nonlinear phase noise is considered, the SNR-limited receiver  $Q$  value can be evaluated by the following equation [9]:

$$Q = \frac{\pi}{2\sqrt{2(\sigma_L^2 + \sigma_{NL}^2)}} \quad (5.4.2)$$

where  $\sigma_L^2$  and  $\sigma_{NL}^2$  are the variance of linear optical amplifier noise and variance of nonlinear phase noise respectively, and they are considered as independent Gaussian noises. The expression of  $\sigma_L^2$  and  $\sigma_{NL}^2$  are as following [12]:

$$\sigma_L^2 = 1/(2 \cdot OSNR) \quad (5.4.3)$$

$$\sigma_{NL}^2 = 2\langle\Phi_{NL}\rangle^2 / (3 \cdot OSNR) \quad (5.4.4)$$

$OSNR$  in Equation (5.4.3) and (5.4.4) is the optical signal-to-noise ratio defined over a matched optical filter with bandwidth of  $B_o$  and can be expressed as:

$$OSNR = P_{in}^{(1)} / (2Nh\omega \cdot NF_{eff} (G_{eff} - 1)B_o) \quad (5.4.5)$$

$\langle\Phi_{NL}\rangle$  in Equation (5.4.3) and (5.4.4) is the accumulated mean nonlinear phase shift and can be expressed as

$$\langle\Phi_{NL}\rangle = N\gamma PL_{eff} \quad (5.4.6)$$

where  $P$  is the signal peak power;  $L_{eff}$  is the effective nonlinear fiber length and its relationship with fiber length  $L$  is:

$$L_{eff} = (1 - \exp(-\alpha L)) / \alpha \quad (5.4.7)$$

with  $\alpha$  being the attenuation of fiber.

Using Equation (5.4.2) to Equation (5.4.7), the SNR-limited transmission distance (at which  $Q$  is reduced to 10) for RZ-DPSK were also calculated and denoted as dashed lines ‘RZ-DPSK, nonlinear’ in Fig. 5.6 (for 10Gb/s) and Fig. 5.7 (for 40Gb/s). Evidently nonlinear phase noise reduces the noise-limited transmission distance at high power levels. In a single-channel 10Gb/s system, as shown in Fig. 5.6 RZ-DPSK modulation format lost its advantage over other modulation formats when nonlinear phase noise is considered, which is consistent with results in Ref. [16]. However, at 40Gb/s as shown in Fig. 5.7, SPM-induced nonlinear waveform distortion is the dominant effect and RZ-DPSK remains the best choice of modulation format even considering the effect of nonlinear phase noise. In practical WDM systems, the conclusion about the selection of modulation formats may be changed for 10Gb/s datarate. When channel spacing in a 10Gb/s system is small, e.g. 25GHz in system like Chapter 4, FWM and XPM may be strong enough to change the selection of modulation formats. For a 40Gb/s WDM system, channel spacing is large enough (e.g. 100GHz), SPM is the dominant degrading effects especially using SSMF. Therefore, RZ-DPSK still is the best choice of the invested modulation formats.

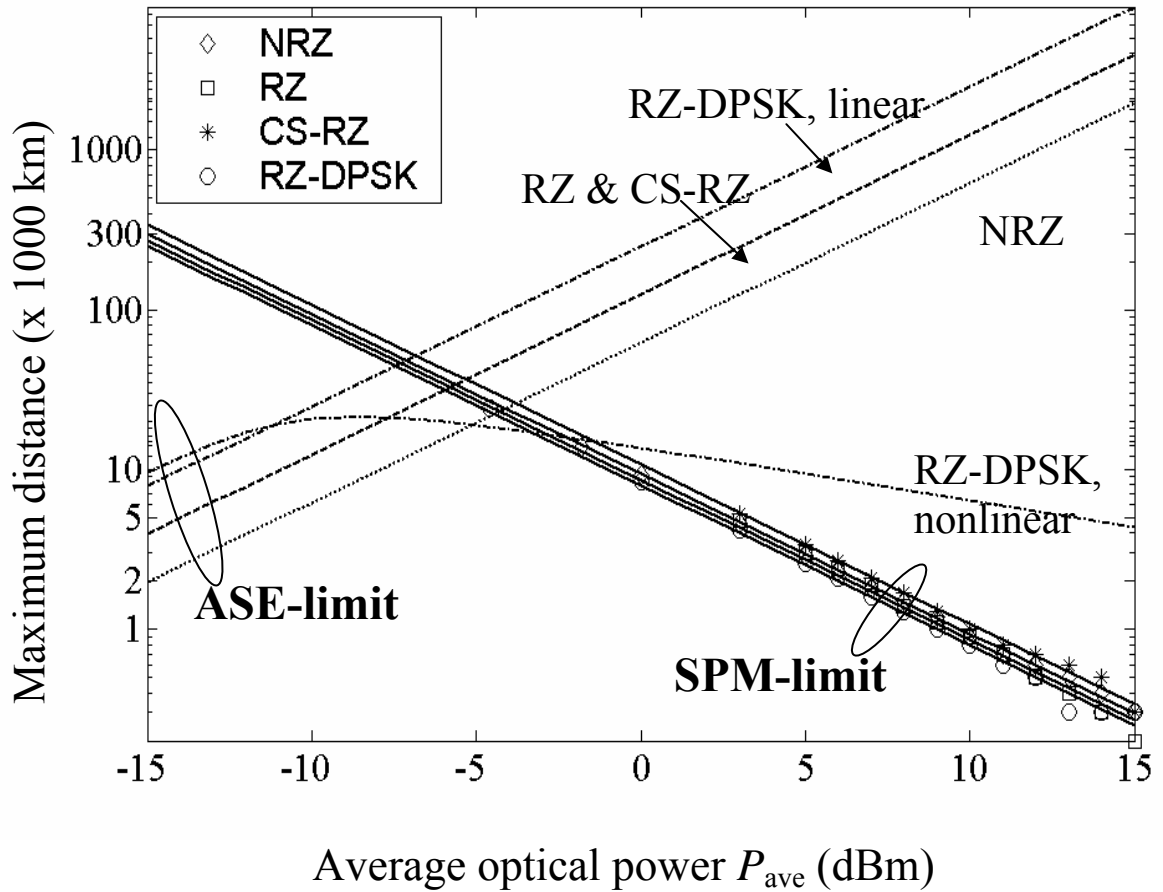


**Fig. 5.6 SPM-limited transmission distance versus launched optical power for 10Gb/s data rate. Scattered points: results of numerical simulations. Solid lines: linear fittings between  $\log(L_{SPM})$  and  $P$ (dBm) with the slope of  $-1$ . Dashed lines: ASE-limited transmission distance from analytical equation.**

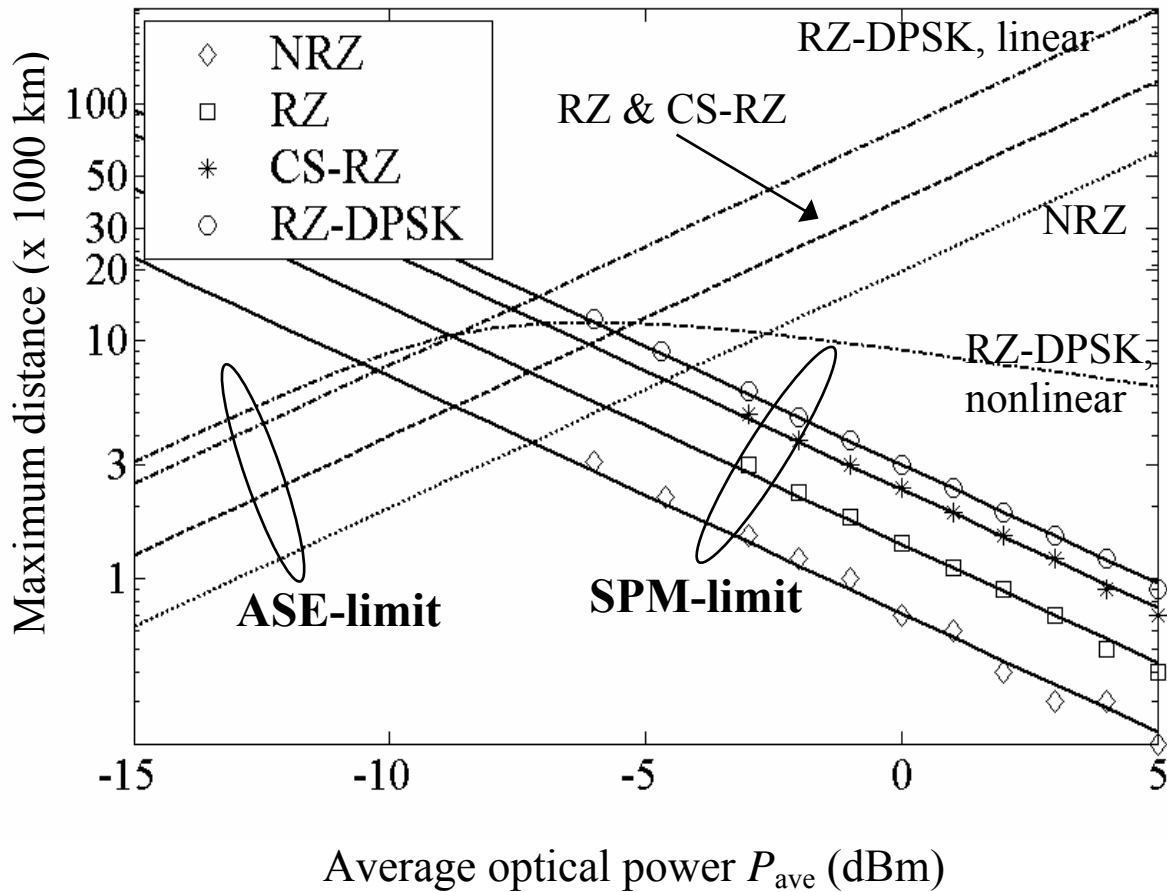


**Fig. 5.7 SPM-limited transmission distance versus launched optical power for 40Gb/s data rate. Scattered points: results of numerical simulations. Solid lines: linear fittings between  $\log(L_{SPM})$  and  $P$ (dBm) with the slope of  $-1$ . Dashed lines: ASE-limited transmission distance from analytical equation.**

## **5.5. Conclusion**

In this chapter, we have investigated the SPM limitation on system performance for dispersion managed optical systems and several optical modulation formats have been compared. A first-order linear relationship between SPM-limited maximum transmission distance and signal optical power is found to be applicable to all the modulation formats investigated. At 40Gb/s datarate, advanced modulation formats such as RZ, CS-RZ and RZ-DPSK have shown improved tolerance to SPM-induced nonlinear distortion compared to the NRZ counterpart.

## **6. 40Gb/s Optical Transmission Testbed**

### **6.1. Motivation**

This chapter is to describe the 40Gb/s optical transmission system established at the Lightwave Communication Laboratory in ITTC. With the development of lightwave systems, 40Gb/s lightwave system has been under intense research. The proposal about its commercial usage has also been brought on the table. It is well known that dispersion compensation and nonlinearity combating are crucial in 40Gb/s system. However there is still a lot of work to understand and to resolve these crucial problems. We develop this testbed for future experimental research on high-speed optical transmission systems and related performance issues. The testbed will also facilitate the research on system performance optimization using advanced optical modulation formats and various types of optical fibers. This experimental capability on 40Gb/s optical transmission systems can be used to validate the theoretical models and simulations; in addition, it will be another way to understand the mechanism under high-speed lightwave telecommunications. In the following part, the description of the high-speed optical transmission testbed will be given first; then, 40Gb/s optical systems with several modulation formats are shown.

### **6.2. 40Gb/s TDM Optical Transmission System Testbed**

Generation of a 40Gb/s optical signal and its bit error measurement is a key issue in the 40Gb/s optical testbed. Usually there are two ways to realize a 40Gb/s optical transmission system: optical domain multiplexing or electrical domain multiplexing and fixed 40Gb/s bit-error test set. Since we already have a 10Gb/s bit

error test set (BERT) at the laboratory, we decide to select electrical domain multiplexing/demultiplexing scheme for the consideration of budget constrain and using of existing equipment as much as possible.

The idea of electrical domain multiplexing/demultiplexing is very straightforward. The 40Gb/s optical testbed using electrical multiplexer/demultiplexer is shown in Fig. 6.1.

In this setup, the key equipment is the 40Gb/s BERT. The 40Gb/s BERT is consisted of one 10Gb/s BERT, one 10G to 40G MUX, and one 40G to 10G DEMUX. The 10Gb/s BERT is the Agilent 10Gb/s BERT we have had for a while. For this setup, we bought MUX and DEMUX from SHF Communications AG.

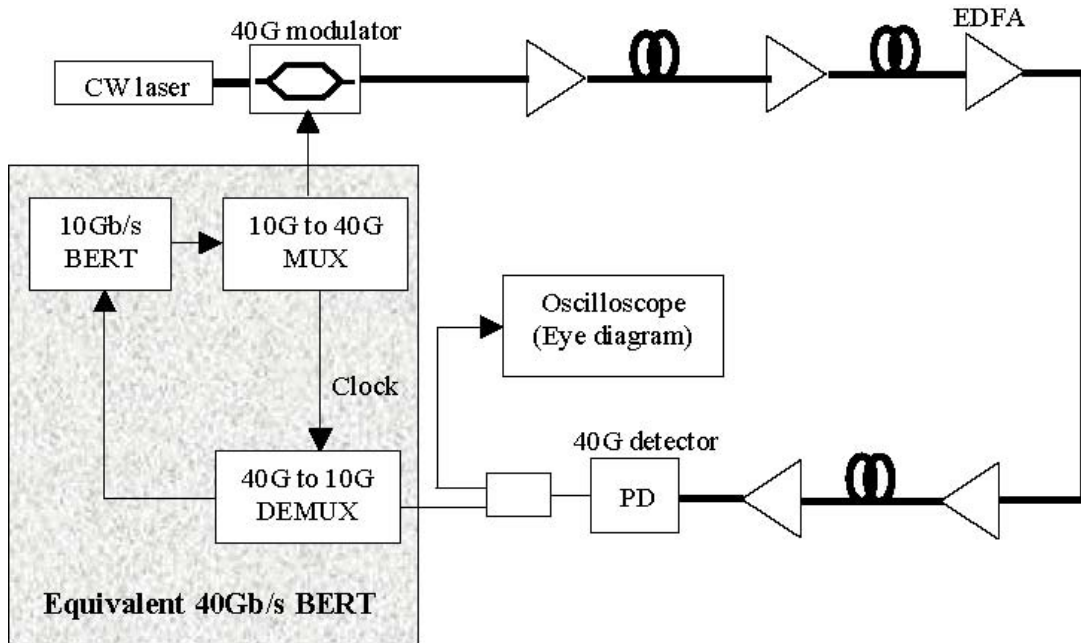


**Fig. 6.1 40Gb/s optical testbed using electrical MUX/DEMUX (Ref. [10])**

At the transmitting end, 10Gb/s BERT serves as a pseudo-random bit pattern generator. As illustrated in Fig. 6.2, a 10Gb/s bit stream is output from the 10Gb/s

BERT, then it is multiplexed into electrical 40Gb/s data rate through the 10G-to-40G MUX. The MUX can split the 10Gb/s PRBS into 4 channels, introduce a relative delay between each of them, reshape the 100ps electrical pulses width into 25ps and then recombine these 4 channels into one 40Gb/s digital output. Although this is essentially a self-multiplexed data pattern and is not a traditional 40Gb/s PRBS, it does serve as a good approximation to a PRBS.

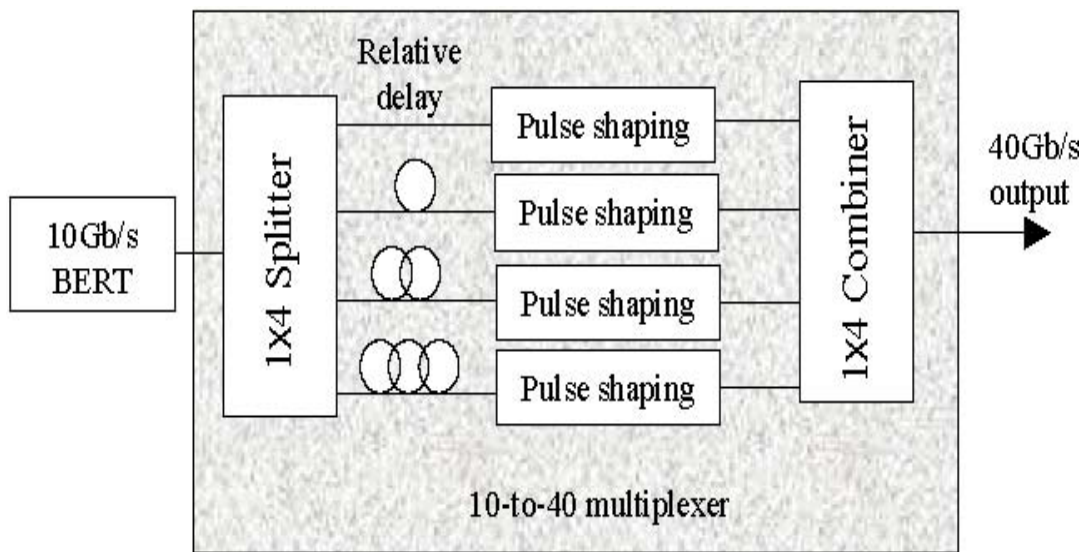


**Fig. 6.2 10G to 40G multiplexing in electrical domain (Ref. [10])**

At the receiving end, a photo diode is used to detect 40Gb/s optical signal. Then, 40Gb/s electrical signal is demultiplexed by the 40G-to-10G DEMUX before it can be detected by the 10Gb/s BERT. 40G-to-10G DEMUX can demultiplex a 40Gb/s data stream into 4 parallel channels of 10Gb/s data streams, and its block diagram is illustrated in Fig. 6.3. Any output channel of 10Gb/s data stream can be used to measure the bit error rate in the following 10Gb/s BERT.

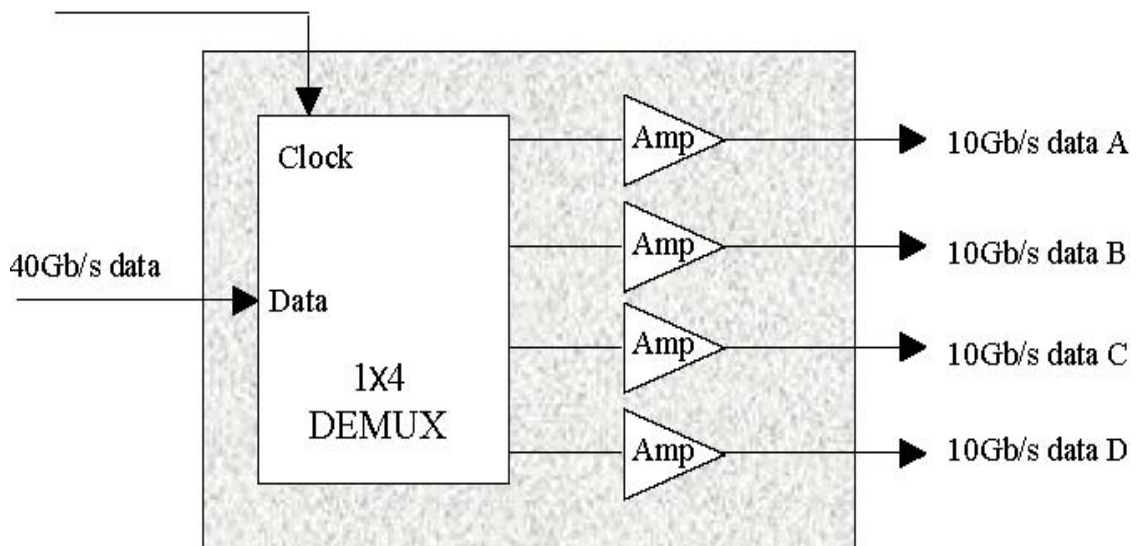
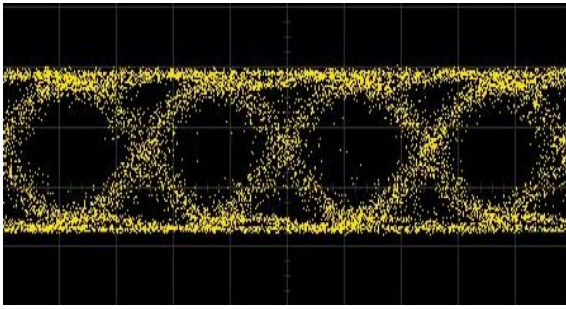


**Fig. 6.3 40G to 10G demultiplexing in electrical domain (Ref. [10])**

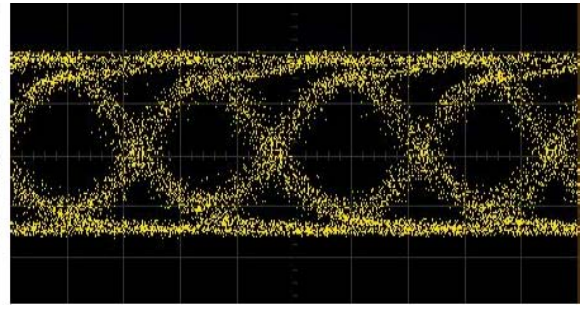
Based on this 40Gb/s BERT, we have evaluated optical systems with NRZ and CS-RZ modulation formats.

### **6.3. 40Gb/s Optical System with NRZ Modulation Format**

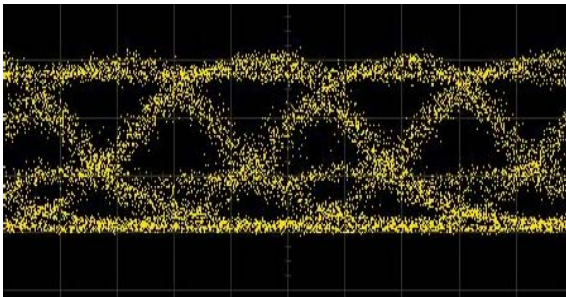
In this system, we use a 1550nm tunable laser as the optical source. A 38GHz bandwidth LiNbO3 electro-optical intensity modulator is directly modulated by the 40Gb/s electrical PRBS data stream to generate a 40Gb/s NRZ optical signal. Examples of 40Gb/s NRZ eye-diagram are shown in Fig. 6.4 for different length of SSMF.



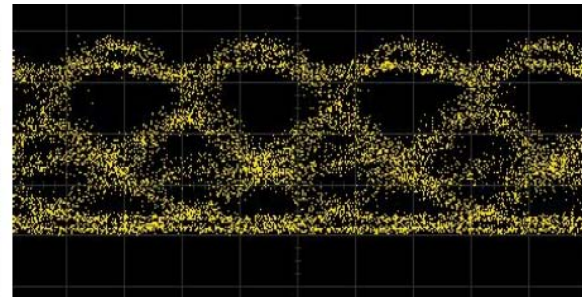
(A) Back-to-back



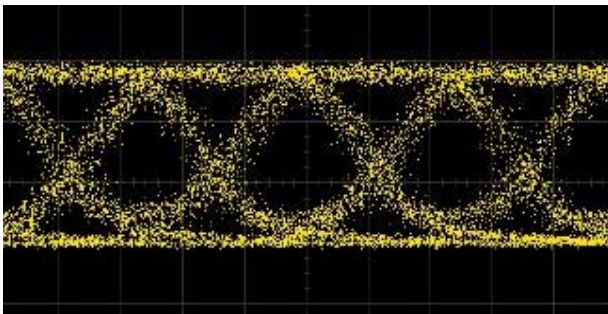
(B) After 2km SMF



(C) After 5km SMF



(D) After 8km SMF



(E) After 10km SMF with 100% dispersion compensation

**Fig. 6.4** Eye diagrams measured at: (A) back-to-back, (B) 2km, (C) 5km and (D) 8km without dispersion compensation; and (E) 10km with dispersion compensation. (Ref. [10])

The dispersion tolerance of a lightwave system is inverse-proportional to the square of datarate. So the transmission distance of a 40Gb/s optical system is 16 times

less than that for a 10Gb/s optical system. Usually a 10Gb/s system can transmit 80km using standard single mode fiber without any dispersion compensation. Therefore, the maximum transmission distance for a 40Gb/s system without dispersion compensation is approximately 5km. Fig. 6.4(C) shows a barely good eye diagram for the transmission length of 5km, and Fig. 6.4(D) clearly shows a severe waveform distortion at fiber length of longer than 5km. When a dispersion compensating fiber is added at the end of the system, the integrity of the waveform is restored and the eye is reopened. And this is shown in Fig. 6.4(E).

NRZ is known for its low tolerance to chromatic dispersion and the stringent requirement on the precision of dispersion compensation. This makes NRZ no more an appropriate modulation format in high speed optical system anymore. In high-speed optical system, e.g. 40Gb/s system, advanced modulation formats should be adopted. Another modulation format we have experimented is CS-RZ.

#### **6.4. 40Gb/s optical system with CS-RZ modulation format**

Since its proposal, CS-RZ modulation format has raised an intense study and has demonstrated better tolerance to chromatic dispersion and signal waveform degradation due to Kerr nonlinear effects.

We have realized a single wavelength CS-RZ optical transmission system. For the detailed information about its waveform generation and characteristics, please refer to Chapter 3. The block diagram of our 40Gb/s CS-RZ experimental system is shown in Fig. 6.5. Two dual-electrode Mach-Zehnder (MZ) modulators are used and

operated in push-pull state. The first MZ modulator has a bandwidth of 38GHz. It was used to encode the 40Gb/s NRZ data directly coming from the 40Gb/s BERT. On the other hand, the second MZ modulator has a bandwidth of 20GHz. It is driven by a 20GHz clock signal. This second modulator is biased at the minimum transmission point as described in Chapter 3.2.5, so that it works as a frequency doubler and generates a 40GHz optical clock with alternating phase between '0' and ' $\pi$ '. So far, 40Gb/s CS-RZ optical signals are generated through two cascading modulators in our experimental testbed. The very distinct feature of CS-RZ is that there is a " $\pi$ " phase difference between adjacent pulses. In another word, the optical field of CS-RZ changes the polarity for every other pulse, and the average optical field would be zero. Therefore, there is no carrier component for the optical field spectrum and the two characteristic frequency components will be at  $\pm 20GHz$ . The measured CS-RZ optical spectrum is shown in Fig. 6.6. However, carrier component is not completely suppressed in the experiment as we can see a small residual carrier component in the measured optical spectrum. The reason for this is that two MZ modulators may not be biased at the optimum point. In practical systems, automatic bias control is required.

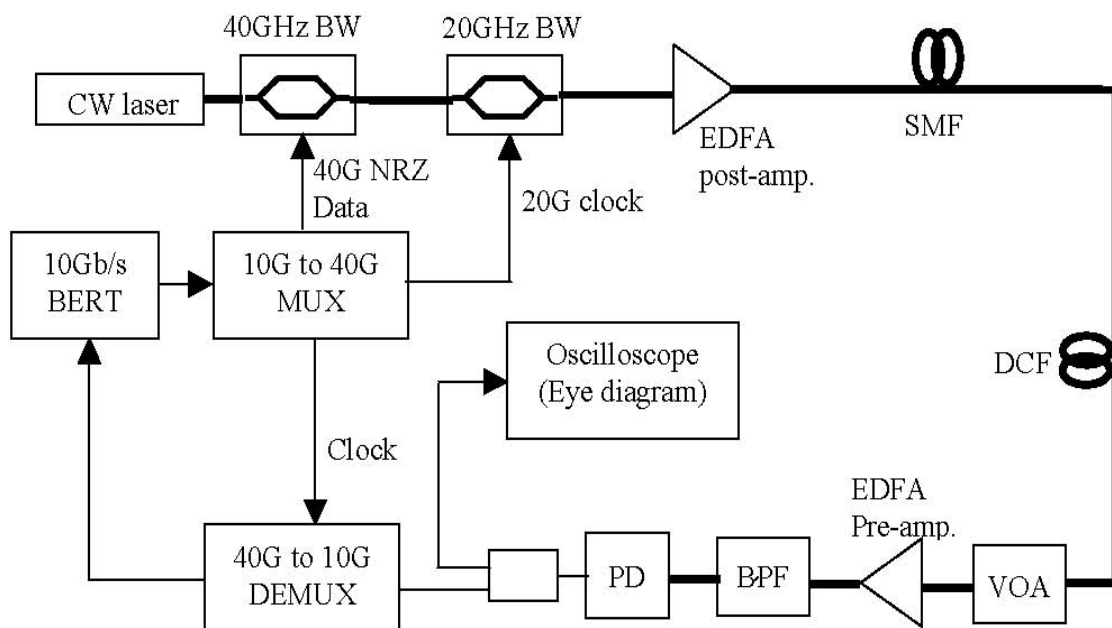


Fig. 6.5 40Gb/s optical system with CS-RZ modulation (Ref. [10])

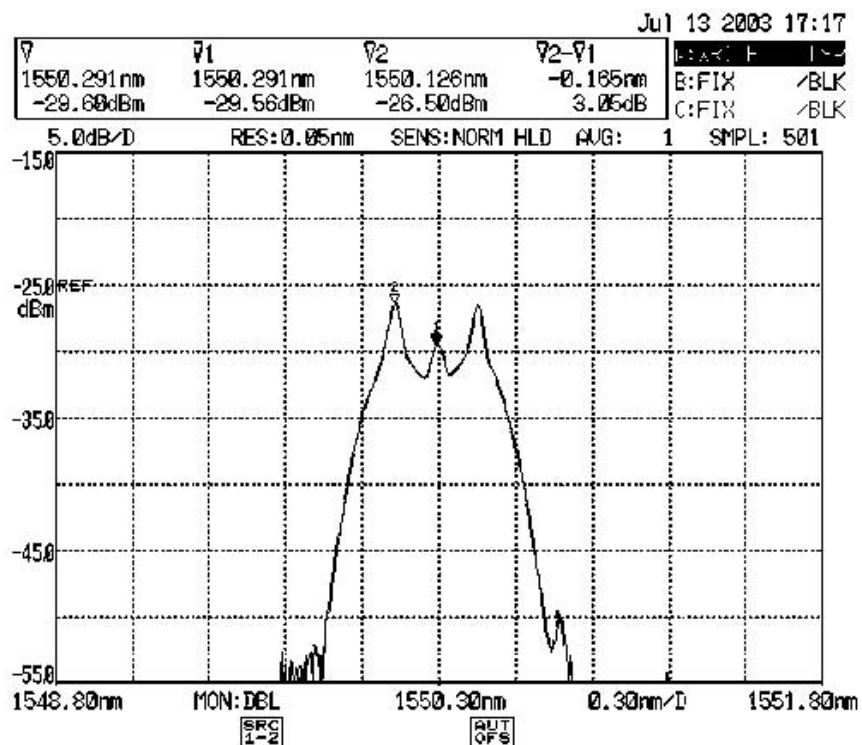
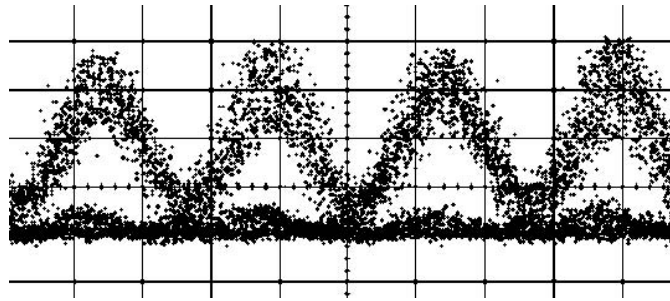


Fig. 6.6 Measured optical spectrum of CS-RZ signal. (Ref. [10])

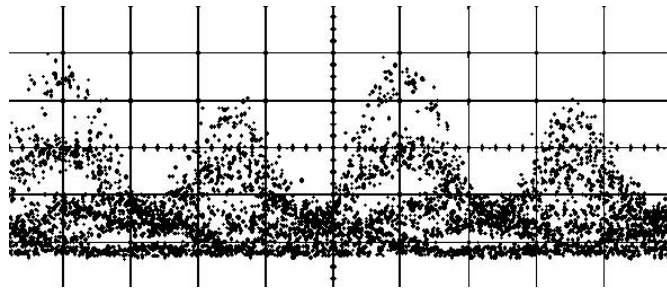
In the experiment, we use Corning SMF28™ fiber with the attenuation of

approximately 0.30dB/km as the transmission fiber, and a length of Lucent DCF with dispersion of  $-164\text{ps/nm}$  for the purpose of dispersion compensating. The laser is tuned at 1532nm with output power of  $-2\text{dBm}$ .

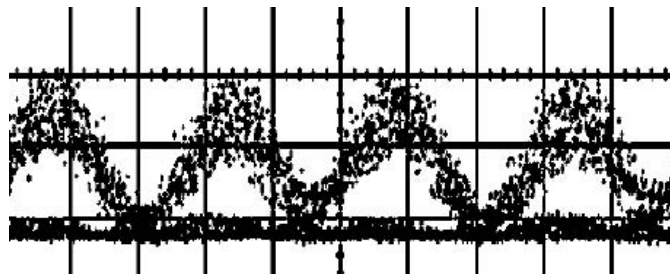
Fig.6.7 shows the measured eye diagrams for back-to-back, over 10km without dispersion compensation and over 10km with dispersion compensation. A variable optical attenuator (VOA) inserted before the EDFA preamplifier, as shown in Fig. 6.5, is used for measuring the receiver sensitivity. In back-to-back operation, the receiver sensitivity is measured as  $-27.9\text{dBm}$  to achieve a  $10^{-9}$  bit-error-rate. For 10km transmission with 100% dispersion compensation, the receiver sensitivity is approximately identical to that in back-to-back operation.



**(A) Back-to-back**



**(B) After 10km without DCF**



**(C) After 10km with DCF**

**Fig. 6.7 CS-RZ eye diagram measured at (A) back-to-back, (B) after 10km SMP without DCF and (C) after 10km with DCF. (Ref. [10])**

## **6.5. Conclusion**

Here, we have demonstrated the experimental capability of a 40Gb/s optical transmission system. Experiments of 40Gb/s transmission with NRZ and CS-RZ

formats have been performed. This testbed provides a foundation for future experimental research on high-speed optical transmission systems and related performance issues. In addition, it will assist on the research of new ideas of high-speed optical transmission and validate theoretical models and numerical results.

## 7. Conclusion and Future Work

In this thesis, we have analyzed several advanced optical modulation formats: NRZ-OOK, RZ-OOK, CS-RZ, NRZ-DPSK and RZ-DPSK. In Chapter1, we have summarized the development of lightwave systems and the importance of optical modulation formats in next generation of lightwave system. In Chapter2, we detailed the waveform generation and detection and major characteristics of each modulation format. In Chapter3, system performance of different modulation formats are compared on different transmission fibers in both 10Gb/s and 40Gb/s WDM systems. It is obvious that the comparison of different modulation format concerning their system performance could be changed when the WDM system has different data rate or channel spacing. In Chapter4, we have derived a first-order rule concerning the SPM degrading effect for different modulation format in a single channel lightwave system with 10Gb/s or 40Gb/s of data rate. This simplified model will decrease the time on system design dramatically. In Chapter5, we have showed the ability to set up a 40Gb/s lightwave testbed. Using this testbed, NRZ and CS-RZ format are realized. The testbed will help to understand the mechanism of optical transmission experimentally and validate the numerical and analyzing results in the near future.

There is still a lot of work to be done in this field.

First of all, there is an increasing attention on multi-level signaling recently, e.g. DQPSK. Multi-level signaling is more efficient than binary signaling. This will definitely increase the capacity of lightwave system. However, it requires a more complex transceiver. The detailed comparison between optimal binary signaling like

DPSK and CS-RZ and multilevel signaling like DQPSK is desired concerning both system performance and commercial realization.

Last, so far, compensation for linear and nonlinear degrading effects is done in optical domain. For example, we use dispersion compensation fiber repeatedly to compensate SPM-CD degrading effect. If we can find a way to compensate linear and nonlinear degrading effects electronically, the system design would be more flexible and more complicated signal processing in electrical domain at transmitter/receiver end would be applied.

## REFERENCES

- [1] Govind P. Agrawal, “Fiber-optic communication systems”, Third edition, 2002
- [2] Govind P. Agrawal, “Nonlinear fiber optics”, Second edition, 1995
- [3] Chidambaram Pavanam, “Vestigial Side Band Demultiplexing for High Spectral Efficiency WDM systems”, *Master thesis submitted to the Department of Electrical Engineering at the University of Kansas*, 2004
- [4] Takeshi Hoshida, Olga Vassilieva, Kaori Yamada, etc. “Optimal 40 Gb/s modulation formats for spectrally efficient long-haul DWDM systems”, *Journal of lightwave technology*, VOL. 20, NO. 12, December 2002
- [5] Yukata Miyamoto, Akira Hirano, Kazushige Yonenaga, etc. “320 Gbit/s (8 x 40Gbit/s) WDM transmission over 367-km zero-dispersion-flattened line with 120-km repeater spacing using carrier-suppressed return-to-zero pulse format”, *OSA TOPS Vol. 30 Optical Amplifiers and their applications*, Jeff C. Livas, Gerlas Van den Hoven and Susumu Kinoshita (eds.) ©1999 Optical Society of America
- [6] Ron Hui, Sen Zhang, etc. “Advanced Optical Modulation Formats and Their Comparison in Fiber-Optic Systems”, *A Technical Report to Sprint*, by *Lightwave Communication Systems Laboratory, The University of Kansas*, 2004
- [7] Sen Zhang, Ron Hui, “Impact of optical modulation formats on SPM-induced limitation in dispersion-managed optical systems – A simplified modeling”, *2004 Workshop on advanced modulation formats, IEEE/LEOS, Paper FA3*, San Francisco, 2004

- [8] O.Vassilieva, T.Hoshida, S. Choudhary, etc. "Numerical comparison of NRZ, CS-RZ and IM-DPSK formats in 43Gbit/s WDM transmission", *Proc. LEOS 14<sup>th</sup> Annual Meeting, paper ThC2*, pp. 673-674, 2001.
- [9] Keang-Po Ho, "Impact of nonlinear phase noise to DPSK signals: A comparison of different models", *IEEE photonics technology letters, VOL. 16, NO. 5*, pp. 1403-1405, May 2004
- [10] Ron Hui, Sen Zhang, Ashvini Ganesh, Chris Allen and Ken Demarest, "40Gb/s Optical Transmission System Testbed", *Technical report, ITTC, the University of Kansas*, January 2004
- [11] R. Billington, "A Report of Four-Wave Mixing in Optical Fibre and its Metrological Applications", NPL Report COEM 24, ISSN COEM 1369-6807, National physical laboratory, Queens Road, Teddington, Middlesex, TW11 0LW, January 1999
- [12] J. P. Gordon, L. F. Mollenauer, "Phase noise in photonic communications systems using linear amplifiers", *Optics letters, Vol. 15, No. 23*, pp. 1351-1353, December, 1990
- [13] Chris Xu, Xiang Liu, Linn F. Mollenauer, and Xing Wei, "Comparison of return-to-zero differential phase-shift keying and on-off keying in long-haul dispersion managed transmission", *IEEE photonics technology letters, VOL. 15, NO. 4*, pp. 617-619, April 2003,

- [14] A.R. Chraplyvy, R.W. Tkach, "What is the actual capacity of single-mode fibers in amplified lightwave systems?", *IEEE photonics letters*, VOL 5, NO. 6, pp. 666-668, June 1993
- [15] Jörg-Peter Elbers, Andreas Färbert, Christian Scheerer etc., "Reduced model to describe SPM-limited fiber transmission in dispersion-managed lightwave systems", *IEEE journal of selected topics in quantum electronics*, VOL. 6. NO. 2, pp. 276-281, March/April 2000
- [16] Takashi Mizuochi, Kazuyuki Ishida, Tatsuya Kobayaashi etc., "A comparative Study of DPSK and OOK WDM Transmission Over Transoceanic Distances and Their Performance Degradations Due to Nonlinear Phase Noise", *Journal of Lightwave Technology*, VOL. 21, NO. 9, pp. 1933-1943, September 2003
- [17] Hoon Kim, Alan H. Gnauck, "Experimental Investigation of the Performance Limitation of DPSK Systems Due to Nonlinear Phase Noise", *IEEE Photonics Technology Letter*, VOL. 15, NO.2, pp. 320-322, February 2003
- [18] Anes Hodžić, Beate Knorad, and Klaus Petermann, "Alternative Modulation Formats in  $N \times 40\text{Gb/s}$  WDM Standard Fiber RZ-Transmission Systems", *Journal of Lightwave Technology*, VOL. 20, NO. 4, pp. 598-607, April 2002
- [19] Yutaka Miyamoto, Tomoyoshi Kataoka, Kazushige Yonenaga etc., "WDM Field Trials of 43-Gb/s/Channel Transport System for Optical Transport Network", *Journal of Lightwave Technology*, VOL. 20, NO.12, pp.2115-2128, December 2002